A NEW WENO-2r ALGORITHM WITH PROGRESSIVE ORDER OF ACCURACY CLOSE TO DISCONTINUITIES*

SERGIO P. AMAT†, JUAN RUIZ‡, CHI-WANG SHU§, AND DIONISIO F. YÁÑEZ¶

Abstract. In this article a modification of the algorithm for data discretized in the point values introduced in [S. Amat, J. Ruiz, and C.-W. Shu, *Appl. Math. Lett.*, 105 (2020), pp. 106–298] is presented. In the aforementioned work, the authors managed to obtain an algorithm that reaches a progressive and optimal order of accuracy close to discontinuities for WENO-6. For higher orders, i.e., WENO-8, WENO-10, etc., it turns out that the previous algorithm presents some *shadows* in the detection of discontinuities, meaning that the order of accuracy is better than the one attained by WENO of the same order, but not optimal. In this article a modification of the smoothness indicators used in the original algorithm is presented. It is oriented to solve this problem and to attain a WENO-2r algorithm with progressive order of accuracy close to the discontinuities. We also show proofs for the accuracy and explicit formulas for all the weights used for any order 2r of the algorithm.

Key words. WENO-2r, high accuracy interpolation, improved adaption to discontinuities, generalization

AMS subject classifications. 41A05, 41A10, 65D05, 65M06, 65N06

DOI. 10.1137/20M1337090

1. Introduction: Classical WENO algorithm. WENO (weighted essentially nonoscillatory) algorithm [1, 2, 3, 4, 5, 6, 7, 8, 9, 10] was designed to use the stencil of the ENO (essentially nonoscillatory) algorithm [11, 12] and to behave in a similar way close to discontinuities, while improving the accuracy at smooth zones. WENO is written using a convex combination of all the interpolating polynomials that share the central interval of the global stencil used. In order to provide an adaptive approximation, the weights of the combination are nonlinear and based on an efficient estimation of the smoothness of each substencil using what are called *smoothness indicators* [2]. In [13] we aimed to provide a WENO-6 algorithm with improved accuracy close to singularities, while keeping the maximum possible accuracy at smooth zones. In the past, some attempts have been made to generalize the work in [13] but without providing satisfactory proofs about the accuracy of the algorithm for any r or explicit

†Departamento de Matemática Aplicada y Estadística, Universidad Politécnica de Cartagena, Cartagena, 30203, Spain (sergio.amat@upct.es).
‡Corresponding author. Departamento de Matemática Aplicada y Estadística, Universidad Politécnica de Cartagena, Cartagena, 30203, Spain (juan.ruiz@upct.es).
§Division of Applied Mathematics, Brown University, Providence, RI 02912 USA (chi-wang_shu@brown.edu).
¶Departamento de Matemáticas, Facultad de Matemáticas, Universidad de Valencia, Valencia, 46100, Spain (dionisio.yanez@uv.es).

expressions for the weights or the smoothness indicators [14, 15]. It is known that the WENO algorithm does not attain the maximum possible accuracy close to discontinuities when there is more than one smooth substencil. Although improving the accuracy of the classical WENO algorithm close to discontinuities, we find that the technique presented in [14] does not attain the maximum possible accuracy at some intervals when r grows. In this article we solve this problem using a simple strategy that has to do with the design of the smoothness indicators of high order and we proof the accuracy of the new algorithm in general. We also give explicit formulas for all the weights used in the algorithm for any r. Finally, we particularize the proofs for low values of r that are most used in practice.

Let's now introduce how the WENO algorithm works. Let X be a uniform partition of the interval $[a, b]$ in J subintervals,

$$X = \{x_i\}_{i=0}^{J}, \quad x_i = a + i \cdot h, \quad h = \frac{b - a}{J}.$$

The point value discretization of the piecewise smooth function f is considered at the nodes x_i,

$$(1) \qquad f_i = f(x_i), \, i = 0, \ldots, J, \quad f = \{f_i\}_{i=0}^{J},$$

and it is supposed that discontinuities are located far enough from each other, meaning that in a stencil only one discontinuity can be found.

In order to interpolate in the interval (x_{i-1}, x_i), the WENO-2r algorithm uses the stencil $\{x_{i-r}, \ldots, x_{i+r-1}\}$, that is composed of 2$r$ nodes. Using the previous stencil, the convex combination

$$(2) \qquad \mathcal{I}(x; f) = \sum_{k=0}^{r-1} \omega_k^r p_k^r(x)$$

can be constructed, with the positive weights $\omega_k^r \geq 0$, $k = 0, \ldots, r-1$, and ensuring that $\sum_{k=0}^{r-1} \omega_k^r = 1$. In expression (2), the rth degree interpolation polynomials are denoted by $p_k^r(x)$. Then, the interpolation at the midpoint of the interval (x_{i-1}, x_i) can be constructed and it will be denoted as $x_{i-\frac{1}{2}}$,

$$(3) \qquad \mathcal{I}(x_{i-\frac{1}{2}}; f) = \sum_{k=0}^{r-1} \omega_k^r p_k^r\left(x_{i-\frac{1}{2}}\right).$$

The values of the ω_k^r are forced to be those that allow us to obtain order of accuracy 2r at $x_{i-\frac{1}{2}}$ when the stencil is smooth. When interpolating the discretized function $\{f(x_i)\}_{i=0}^{2r}$, the objective is to obtain an interpolation polynomial that satisfies

$$p_0^{2r-1}\left(x_{i-\frac{1}{2}}\right) = f\left(x_{i-\frac{1}{2}}\right) + O(h^{2r}),$$

based on the big stencil $\{x_{i-r}, \ldots, x_{i+r-1}\}$, through the convex combination of the r consecutive interpolation polynomials of order r,

$$p_k^r\left(x_{i-\frac{1}{2}}\right) = f\left(x_{i-\frac{1}{2}}\right) + O(h^{r+1}).$$

Now, the classical WENO algorithm and its properties can be reviewed. The classical WENO-2r interpolator, $\bar{\mathcal{I}}(x; f)$, imposes that the optimal weights are $\bar{C}_k^r \geq 0$, with $k = 0, \ldots, r-1$, and $\sum_{k=0}^{r-1} \bar{C}_k^r = 1$, such that

$$(4) \qquad p_0^{2r-1}\left(x_{i-\frac{1}{2}}\right) = \sum_{k=0}^{r-1} \bar{C}_k^r p_k^r\left(x_{i-\frac{1}{2}}\right).$$

A formula for the optimal weights is obtained in [4],

$$(5) \qquad \bar{C}_k^r = \frac{1}{2^{2r-1}}\binom{2r}{2k+1}, \quad k = 0, \ldots, r-1.$$

The weights $\bar{\omega}_k^r$ are designed [1] in order to satisfy at smooth zones that

$$(6) \qquad \bar{\omega}_k^r = \bar{C}_k^r + O(h^\kappa), \quad k = 0, \ldots, r-1,$$

with $\kappa \le r-1$, ensuring that the interpolation in (3) attains order of accuracy $2r$ when $\kappa = r-1$, and

$$(7) \qquad f\left(x_{i-\frac{1}{2}}\right) - \bar{\mathcal{I}}\left(x_{i-\frac{1}{2}}; f\right) = O\left(h^{r+\kappa+1}\right),$$

that matches the accuracy attained by the interpolation polynomial $p_0^{2r-1}(x)$ of $2r$ points. In [1, 2] the authors propose the following expressions for the nonlinear weights:

$$(8) \qquad \bar{\omega}_k^r = \frac{\bar{\alpha}_k^r}{\sum_{j=0}^{r-1} \bar{\alpha}_j^r}, \quad \text{where } \bar{\alpha}_k^r = \frac{\bar{C}_k^r}{(\epsilon + \bar{I}_k^r)^t}, \quad k = 0, \ldots, r-1,$$

with $\sum_{k=0}^{r-1} \bar{\omega}_k^r = 1$. In the previous expression, the parameter t is an integer that ensures maximum order of accuracy close to the discontinuities. The parameter $\epsilon > 0$ is introduced to avoid divisions by zero and is usually forced to take the size of the smoothness indicators at smooth zones. In our numerical tests, we will set it to $\epsilon = 10^{-16}$ (although greater values can be chosen). The values $\bar{I}_k^r$ are called *smoothness indicators* for $f(x)$ on each substencil of r points. The expression for the $\bar{I}_k^r$ initially given in [4] is

$$(9) \qquad \bar{I}_k^r = \sum_{l=1}^{r-1} h^{2l-1} \int_{x_{i-1}}^{x_i} \left(\frac{d^l}{dx^l} p_k^r(x)\right)^2 dx.$$

As shown in [16], these smoothness indicators are only capable of detecting jumps in the function but not in the first derivative. Thus, in section 4 the smoothness indicators chosen for our algorithm are explained.

In this paper, we generalize and improve the algorithms presented in [14, 13] achieving maximum order of accuracy in the intervals close to the discontinuities for any value of r. We introduce the notation and review the previous results in section 2. In order to design the new algorithm, the optimal and nonlinear weights are presented in section 3. Afterward, new smoothness indicators and their properties are proved in section 4. In section 5, we analyze the accuracy of the new method, and finally we perform some experiments comparing the new method with the classical WENO and the new method in section 6. Finally, section 7 is dedicated to presenting the conclusions.

2. Review of previous results: The cases $r = 3$ and $r = 4$. In [14, 13] a new WENO-$2r$ algorithm was presented that improves the resolution of classical WENO algorithms close to discontinuities. For WENO-6, i.e., r = 3, the pattern of

accuracy obtained with the new algorithm was $\ldots, O(h^6), O(h^5), O(h^4), O(1), O(h^4),$ $O(h^5), O(h^6), \ldots$, that is the optimal accuracy that can be expected in the presence of a singularity (the one obtained by the classical WENO is typically $\ldots, O(h^6),$ $O(h^4), O(h^4), O(1), O(h^4), O(h^4), O(h^6), \cdots$). For higher orders, i.e., $r = 4, 5, \ldots$, and despite the fact that the new algorithm obtains a better accuracy than the classical WENO algorithm close to discontinuities, the theoretical pattern of accuracy obtained was not optimal, being for $r = 4, \ldots, O(h^8), O(h^7), O(h^5), O(h^5), O(1), O(h^5), O(h^5),$ $O(h^7), O(h^8) \ldots$, or for $r = 5, \ldots, O(h^{10}), O(h^9), O(h^6), O(h^6), O(h^6), O(1), O(h^6),$ $O(h^6), O(h^6), O(h^9), O(h^{10}) \cdots$, and so on.

The construction proposed in [14] was based on a progressive construction of the building polynomials of the WENO algorithm. This construction was based upon the observation that Lagrange interpolating polynomials of high order can be constructed from polynomials of lower order using a dyadic architecture. For example, for $r = 3$ (stencil of six points) the polynomials of degree 3, $p_0^3(x), p_1^3(x)$, and $p_2^3(x)$ can be used to write polynomials of degree 4. For a stencil of six points there exist two different Lagrange interpolating polynomials of degree 4 (stencil of five points) and will be noted as $p_0^4(x), p_1^4(x)$. There also exists one polynomial of degree 5 (stencil of six points) that will be noted as $p_0^5(x)$. Now, it is clear that we can proceed to construct the polynomials of degree 4 using the polynomials of degree 3 as building blocks; the following notation is used:

$$(10) \quad \begin{aligned} p_0^4\left(x_{i-\frac{1}{2}}\right) &= C_{0,0}^3 p_0^3\left(x_{i-\frac{1}{2}}\right) + C_{0,1}^3 p_1^3\left(x_{i-\frac{1}{2}}\right) = \frac{3}{8}p_0^3\left(x_{i-\frac{1}{2}}\right) + \frac{5}{8}p_1^3\left(x_{i-\frac{1}{2}}\right), \\ p_1^4\left(x_{i-\frac{1}{2}}\right) &= C_{1,1}^3 p_1^3\left(x_{i-\frac{1}{2}}\right) + C_{1,2}^3 p_2^3\left(x_{i-\frac{1}{2}}\right) = \frac{5}{8}p_1^3\left(x_{i-\frac{1}{2}}\right) + \frac{3}{8}p_2^3\left(x_{i-\frac{1}{2}}\right). \end{aligned}$$

And we use the polynomials of degree 4 as building blocks to construct the polynomial of degree 5,

$$(11) \quad p_0^5\left(x_{i-\frac{1}{2}}\right) = C_{0,0}^4 p_0^4\left(x_{i-\frac{1}{2}}\right) + C_{0,1}^4 p_1^4\left(x_{i-\frac{1}{2}}\right) = \frac{1}{2}p_0^4\left(x_{i-\frac{1}{2}}\right) + \frac{1}{2}p_1^4\left(x_{i-\frac{1}{2}}\right).$$

Once this point is reached, in [14] it is proposed to use the vectors of optimal weights $\mathbf{C_0^4}, \mathbf{C_1^4}$ in the classical WENO algorithm. These vectors have as coordinates the weights in (10),

$$(12) \quad \begin{aligned} \mathbf{C_0^4} &= \left(C_{0,0}^3, C_{0,1}^3, 0\right) = \left(\frac{3}{8}, \frac{5}{8}, 0\right), \\ \mathbf{C_1^4} &= \left(0, C_{1,1}^3, C_{1,2}^3\right) = \left(0, \frac{5}{8}, \frac{3}{8}\right). \end{aligned}$$

The stencil used in this case is composed of data at the positions $\{x_{i-3}, x_{i-2}, x_{i-1}, x_i,$ $x_{i+1}, x_{i+2}\}$. It is clear that it is convenient to use $\mathbf{C_0^4}$ when there is a discontinuity placed in (x_{i+1}, x_{i+2}) and $\mathbf{C_1^4}$ if it is placed in the interval (x_{i-3}, x_{i-2}). The objective is to obtain the weights in (5) for $r = 3$ if the stencil does not contain any discontinuities, so that maximum accuracy is attained everywhere. In [14] the weighted average of the vectors in (12) is proposed:

$$(13) \quad \begin{aligned} C_{0,0}^4 \mathbf{C_0^4} + C_{0,1}^4 \mathbf{C_1^4} &= \frac{1}{2}\mathbf{C_0^4} + \frac{1}{2}\mathbf{C_1^4} = \frac{1}{2}\left(\frac{3}{8}, \frac{5}{8}, 0\right) + \frac{1}{2}\left(0, \frac{5}{8}, \frac{3}{8}\right) \\ &= \left(\frac{3}{16}, \frac{10}{16}, \frac{3}{16}\right) = \left(\bar{C}_0^3, \bar{C}_1^3, \bar{C}_2^3\right) = \bar{\mathbf{C}}^3. \end{aligned}$$

The reader can observe how the construction reminds us a WENO algorithm that is computed in several steps in order to grow one at a time the accuracy of the final interpolant. The obvious pace leads us to define nonlinear weights for replacing the constant weights in (13). The weights can be written as

$$(14) \qquad \tilde{\omega}_{0,0}^4 = \frac{\tilde{\alpha}_{0,0}^4}{\tilde{\alpha}_{0,0}^4 + \tilde{\alpha}_{0,1}^4}, \quad \tilde{\omega}_{0,1}^4 = \frac{\tilde{\alpha}_{0,1}^4}{\tilde{\alpha}_{0,0}^4 + \tilde{\alpha}_{0,1}^4},$$

with

$$(15) \qquad \tilde{\alpha}_{0,0}^4 = \frac{C_{0,0}^4}{(\epsilon + \tilde{I}_{0,0}^4)^t} = \frac{1/2}{(\epsilon + \tilde{I}_{0,0}^4)^t}, \quad \tilde{\alpha}_{0,1}^4 = \frac{C_{0,1}^4}{(\epsilon + \tilde{I}_{0,1}^4)^t} = \frac{1/2}{(\epsilon + \tilde{I}_{0,1}^4)^t}.$$

The result of this process is an expression for the adapted optimal weights of the classical WENO algorithm that ensure optimal accuracy for $r = 3$ and that replace the classical constant optimal weights $\bar{C}_k^r$ in (8),

$$(16) \qquad \tilde{\mathbf{C}}^3 = (\tilde{C}_0^3, \tilde{C}_1^3, \tilde{C}_2^3) = \tilde{\omega}_{0,0}^4 \mathbf{C}_0^4 + \tilde{\omega}_{0,1}^4 \mathbf{C}_1^4.$$

The smoothness indicators $\tilde{I}_{0,k_1}^4$, $k_1 = 0, 1$ in (15) will be defined in section 4 based on those introduced in [13, 16], which work well for detecting kinks and jumps in the function if the data is discretized in the point values (1). Thus, finally, the WENO algorithm can be applied with the new nonlinear weights:

$$\tilde{\mathcal{I}}(x_{i-\frac{1}{2}}; f) = \sum_{k=0}^2 \tilde{\omega}_k^3 p_k^3 \left(x_{i-\frac{1}{2}} \right)$$

with

$$(17) \qquad \tilde{\omega}_k^3 = \frac{\tilde{\alpha}_k^3}{\sum_{j=0}^2 \tilde{\alpha}_j} \quad \text{and} \quad \tilde{\alpha}_k^3 = \frac{\tilde{C}_k^3}{(\epsilon + \tilde{I}_k^3)^t}, \quad k = 0, 1, 2,$$

where $\tilde{I}_k^3$, $k = 0, 1, 2$, are the smoothness indicators proposed in [16].

For $r = 4$ and higher values of r, it is possible to follow similar steps. In order to design the new WENO-8 algorithm, a stencil of eight points composed of data placed at the positions $\{x_{i-4}, x_{i-3}, x_{i-2}, x_{i-1}, x_i, x_{i+1}, x_{i+2}, x_{i+3}\}$ is chosen. In this case there exist four polynomials of degree 4 (stencil of five points), which will be noted by $p_0^4(x), p_1^4(x), p_2^4(x), p_3^4(x)$, three of degree 5 (stencil of six points), denoted by $p_0^5(x), p_1^5(x), p_2^5(x)$, two of degree 6 (stencil of seven points), denoted as $p_0^6(x), p_1^6(x)$, and one of degree 7 (stencil of eight points), denoted as $p_0^7(x)$. The process is similar as before: obtain nonlinear optimal weights that ensure the optimal accuracy that the data of the stencil provides. As already done for $r = 3$, the polynomials of degree 5 are written using the polynomials of degree 4 as building blocks,

$$(18) \quad p_0^5\left(x_{i-\frac{1}{2}}\right) = C_{0,0}^4 p_0^4\left(x_{i-\frac{1}{2}}\right) + C_{0,1}^4 p_1^4\left(x_{i-\frac{1}{2}}\right) = \frac{3}{10}p_0^4\left(x_{i-\frac{1}{2}}\right) + \frac{7}{10}p_1^4\left(x_{i-\frac{1}{2}}\right),$$

$$p_1^5\left(x_{i-\frac{1}{2}}\right) = C_{1,1}^4 p_1^4\left(x_{i-\frac{1}{2}}\right) + C_{1,2}^4 p_2^4\left(x_{i-\frac{1}{2}}\right) = \frac{1}{2}p_1^4\left(x_{i-\frac{1}{2}}\right) + \frac{1}{2}p_2^4\left(x_{i-\frac{1}{2}}\right),$$

$$p_2^5\left(x_{i-\frac{1}{2}}\right) = C_{2,2}^4 p_2^4\left(x_{i-\frac{1}{2}}\right) + C_{2,3}^4 p_3^4\left(x_{i-\frac{1}{2}}\right) = \frac{7}{10}p_2^4\left(x_{i-\frac{1}{2}}\right) + \frac{3}{10}p_3^4\left(x_{i-\frac{1}{2}}\right).$$

The polynomials of degree 6 can be written using the polynomials of degree 5 as building blocks,

$$(19) \quad \begin{aligned} p_0^6\left(x_{i-\frac{1}{2}}\right) &= C_{0,0}^5 p_0^5\left(x_{i-\frac{1}{2}}\right) + C_{0,1}^5 p_1^5\left(x_{i-\frac{1}{2}}\right) = \frac{5}{12}p_0^5\left(x_{i-\frac{1}{2}}\right) + \frac{7}{12}p_1^5\left(x_{i-\frac{1}{2}}\right), \\ p_1^6\left(x_{i-\frac{1}{2}}\right) &= C_{1,1}^5 p_1^5\left(x_{i-\frac{1}{2}}\right) + C_{1,2}^5 p_2^5\left(x_{i-\frac{1}{2}}\right) = \frac{7}{12}p_1^5\left(x_{i-\frac{1}{2}}\right) + \frac{5}{12}p_2^5\left(x_{i-\frac{1}{2}}\right). \end{aligned}$$

In this last step, the polynomial of degree 7 is written in terms of the two polynomials of degree 6,

$$(20) \quad p_0^7\left(x_{i-\frac{1}{2}}\right) = C_{0,0}^6 p_0^6\left(x_{i-\frac{1}{2}}\right) + C_{0,1}^6 p_1^6\left(x_{i-\frac{1}{2}}\right) = \frac{1}{2}p_0^6\left(x_{i-\frac{1}{2}}\right) + \frac{1}{2}p_1^6\left(x_{i-\frac{1}{2}}\right).$$

In a similar fashion as done for $r = 3$, the vectors of weights $\mathbf{C_0^5}, \mathbf{C_1^5}, \mathbf{C_2^5}$ can be obtained. They will have as coordinates the constant weights in (18),

(21)
$$\mathbf{C_0^5} = \left(C_{0,0}^4, C_{0,1}^4, 0, 0\right) = \left(\frac{3}{10}, \frac{7}{10}, 0, 0\right), \quad \mathbf{C_1^5} = \left(0, C_{1,1}^4, C_{1,2}^4, 0\right) = \left(0, \frac{1}{2}, \frac{1}{2}, 0\right),$$
$$\mathbf{C_2^5} = \left(0, 0, C_{2,2}^4, C_{2,3}^4\right) = \left(0, 0, \frac{7}{10}, \frac{3}{10}\right).$$

Now, the previous vectors are multiplied by the constant weights calculated in (19) and (20) to obtain the weights that ensure optimal accuracy at smooth zones. These weights are the constant optimal weights used by the classical WENO-8 algorithm, i.e.,

$$(22) \quad \begin{aligned} &C_{0,0}^6\left(C_{0,0}^5\mathbf{C_0^5} + C_{0,1}^5\mathbf{C_1^5}\right) + C_{0,1}^6\left(C_{1,1}^5\mathbf{C_1^5} + C_{1,2}^5\mathbf{C_2^5}\right) \\ &= \frac{1}{2}\left(\frac{5}{12}\mathbf{C_0^5} + \frac{7}{12}\mathbf{C_1^5}\right) + \frac{1}{2}\left(\frac{7}{12}\mathbf{C_1^5} + \frac{5}{12}\mathbf{C_2^5}\right) \\ &= \left(\frac{1}{16}, \frac{7}{16}, \frac{7}{16}, \frac{1}{16}\right) \\ &= \left(\bar{C}_0^4, \bar{C}_1^4, \bar{C}_2^4, \bar{C}_3^4\right) = \bar{\mathbf{C}}^4. \end{aligned}$$

It is clear that the constant weights in (22) can be replaced by nonlinear weights. As before, they will be represented by $\tilde{\omega}_{k,k_1}^l$, $5 \le l \le 6$ and $0 \le k \le 6-l$, $k_1 = k, k+1$. The nonlinear weights are

(23)
$$\tilde{\omega}_{0,0}^5 = \frac{\tilde{\alpha}_{0,0}^5}{\tilde{\alpha}_{0,0}^5 + \tilde{\alpha}_{0,1}^5}, \quad \tilde{\omega}_{0,1}^5 = \frac{\tilde{\alpha}_{0,1}^5}{\tilde{\alpha}_{0,0}^5 + \tilde{\alpha}_{0,1}^5}, \quad \tilde{\omega}_{1,1}^5 = \frac{\tilde{\alpha}_{1,1}^5}{\tilde{\alpha}_{1,1}^5 + \tilde{\alpha}_{1,2}^5}, \quad \tilde{\omega}_{1,2}^5 = \frac{\tilde{\alpha}_{1,2}^5}{\tilde{\alpha}_{1,1}^5 + \tilde{\alpha}_{1,2}^5},$$
$$\tilde{\omega}_{0,0}^6 = \frac{\tilde{\alpha}_{0,0}^6}{\tilde{\alpha}_{0,0}^6 + \tilde{\alpha}_{0,1}^6}, \quad \tilde{\omega}_{0,1}^6 = \frac{\tilde{\alpha}_{0,1}^6}{\tilde{\alpha}_{0,0}^6 + \tilde{\alpha}_{0,1}^6},$$

with

(24)
$$\tilde{\alpha}_{0,0}^5 = \frac{C_{0,0}^5}{(\epsilon + \tilde{I}_{0,0}^5)^t}, \quad \tilde{\alpha}_{0,1}^5 = \frac{C_{0,1}^5}{(\epsilon + \tilde{I}_{0,1}^5)^t}, \quad \tilde{\alpha}_{1,1}^5 = \frac{C_{1,1}^5}{(\epsilon + \tilde{I}_{1,1}^5)^t}, \quad \tilde{\alpha}_{1,2}^5 = \frac{C_{1,2}^5}{(\epsilon + \tilde{I}_{1,2}^5)^t},$$
$$\tilde{\alpha}_{0,0}^6 = \frac{C_{0,0}^6}{(\epsilon + \tilde{I}_{0,0}^6)^t}, \quad \tilde{\alpha}_{0,1}^6 = \frac{C_{0,1}^6}{(\epsilon + \tilde{I}_{0,1}^6)^t},$$

which replacing the values of the C_{k,k_1}^l given in (22) result in

(25)

$$\tilde{\alpha}_{0,0}^5 = \frac{5/12}{(\epsilon + \tilde{I}_{0,0}^5)^t}, \quad \tilde{\alpha}_{0,1}^5 = \frac{7/12}{(\epsilon + \tilde{I}_{0,1}^5)^t}, \quad \tilde{\alpha}_{1,1}^5 = \frac{7/12}{(\epsilon + \tilde{I}_{1,1}^5)^t}, \quad \tilde{\alpha}_{1,2}^5 = \frac{5/12}{(\epsilon + \tilde{I}_{1,2}^5)^t},$$

$$\tilde{\alpha}_{0,0}^6 = \frac{1/2}{(\epsilon + \tilde{I}_{0,0}^6)^t}, \quad \tilde{\alpha}_{0,1}^6 = \frac{1/2}{(\epsilon + \tilde{I}_{0,1}^6)^t}.$$

Just as done before, the adapted optimal weights are obtained replacing the fixed weights in (22) by the nonlinear weights in (23),

$$(26) \quad \tilde{\mathbf{C}}^4 = (\tilde{C}_0^4, \tilde{C}_1^4, \tilde{C}_2^4, \tilde{C}_3^4) = \tilde{\omega}_{0,0}^6 \left(\tilde{\omega}_{0,0}^5 \mathbf{C_0^5} + \tilde{\omega}_{0,1}^5 \mathbf{C_1^5} \right) + \tilde{\omega}_{0,1}^6 \left(\tilde{\omega}_{1,1}^5 \mathbf{C_1^5} + \tilde{\omega}_{1,2}^5 \mathbf{C_2^5} \right).$$

The previous expression provides the nonlinear optimal weights $\tilde{C}_k^r$ that are used to replace the optimal weights $\bar{C}_k^r$ in (8) of the classical WENO algorithm. The smoothness indicators that appear in (26) will be defined in section 4. Analogously to the case $r = 3$, the classical WENO algorithm can be applied with the new nonlinear weights:

$$\tilde{\mathcal{I}}(x_{i-\frac{1}{2}}; f) = \sum_{k=0}^3 \tilde{\omega}_k^4 p_k^4 \left(x_{i-\frac{1}{2}} \right)$$

with

$$(27) \qquad \tilde{\omega}_k^4 = \frac{\tilde{\alpha}_k^4}{\sum_{j=0}^3 \tilde{\alpha}_j}, \quad \text{with} \quad \tilde{\alpha}_k^4 = \frac{\tilde{C}_k^4}{(\epsilon + \tilde{I}_k^4)^t}, \quad k = 0, 1, 2, 3,$$

being $\tilde{I}_k^4$, $k = 0, 1, 2, 3$, the smoothness indicators defined in [16, 13].

A generalization of this process for any r can be obtained now. The difficulty lies in constructing smoothness indicators for each level that are able *to watch* the discontinuities correctly. In the next section, we present the generalization of the algorithm for order $2r$ and explicit expressions for all the weights.

3. General explicit expressions for new WENO-2r weights. Following the strategy described in the previous section, a WENO-2r algorithm with optimal accuracy can be constructed for any r. In order to extend the results to any r the following lemma can be used.

LEMMA 3.1. *Let* $r \le l \le 2r - 2$ *and* $0 \le k \le (2r - 2) - l$ *if* $C_{k,k}^l$ *and* $C_{k,k+1}^l$ *are the values which satisfy*

$$(28) \qquad p_k^{l+1} \left(x_{i-\frac{1}{2}} \right) = C_{k,k}^l p_k^l \left(x_{i-\frac{1}{2}} \right) + C_{k,k+1}^l p_{k+1}^l \left(x_{i-\frac{1}{2}} \right),$$

then

$$(29) \qquad C_{k,k}^l = 1 - \frac{2(r-k)-1}{2(l+1)}, \quad C_{k,k+1}^l = 1 - C_{k,k}^l = \frac{2(r-k)-1}{2(l+1)}.$$

Proof. Let $r \le l \le 2r - 2$ and $0 \le k \le (2r - 2) - l$, and the stencils used to obtain the interpolators p_k^{l+1}, p_k^l, and p_{k+1}^l are $\{x_{i-r+k}, \ldots, x_{i-r+k+l+1}\}$, $\{x_{i-r+k}, \ldots, x_{i-r+k+l}\}$, and $\{x_{i-r+k+1}, \ldots, x_{i-r+k+l+1}\}$, respectively; then using Aitken's interpolation process [17], from $x_i = a + ih$, we get

$$p_k^{l+1} \left(x_{i-\frac{1}{2}} \right) = \frac{x_{i-r+k+l+1} - x_{i-\frac{1}{2}}}{x_{i-r+k+l+1} - x_{i-r+k}} p_k^l \left(x_{i-\frac{1}{2}} \right) - \frac{x_{i-r+k} - x_{i-\frac{1}{2}}}{x_{i-r+k+l+1} - x_{i-r+k}} p_{k+1}^l \left(x_{i-\frac{1}{2}} \right)$$

$$= \frac{2(l-r+k+1)+1}{2(l+1)} p_k^l \left(x_{i-\frac{1}{2}} \right) + \frac{2(r-k)-1}{2(l+1)} p_{k+1}^l \left(x_{i-\frac{1}{2}} \right)$$

$$= C_{k,k}^l p_k^l \left(x_{i-\frac{1}{2}} \right) + C_{k,k+1}^l p_{k+1}^l \left(x_{i-\frac{1}{2}} \right). \qquad \square$$

The same construction can be done for any r starting by writing the polynomials of degree $2r - 1$ as a combination of polynomials of degree $2r - 2$,

$$p_0^{2r-1}\left(x_{i-\frac{1}{2}}\right) = C_{0,0}^{2r-2}p_0^{2r-2}\left(x_{i-\frac{1}{2}}\right) + C_{0,1}^{2r-2}p_1^{2r-2}\left(x_{i-\frac{1}{2}}\right),$$

and repeating the process for degree $2r - 2$,

$$p_0^{2r-2}\left(x_{i-\frac{1}{2}}\right) = C_{0,0}^{2r-3}p_0^{2r-3}\left(x_{i-\frac{1}{2}}\right) + C_{0,1}^{2r-3}p_1^{2r-3}\left(x_{i-\frac{1}{2}}\right),$$

$$p_1^{2r-2}\left(x_{i-\frac{1}{2}}\right) = C_{1,1}^{2r-3}p_1^{2r-3}\left(x_{i-\frac{1}{2}}\right) + C_{1,2}^{2r-3}p_2^{2r-3}\left(x_{i-\frac{1}{2}}\right),$$

for degree $2r - 3$,

$$p_0^{2r-3}\left(x_{i-\frac{1}{2}}\right) = C_{0,0}^{2r-4}p_0^{2r-4}\left(x_{i-\frac{1}{2}}\right) + C_{0,1}^{2r-4}p_1^{2r-4}\left(x_{i-\frac{1}{2}}\right),$$

$$p_1^{2r-3}\left(x_{i-\frac{1}{2}}\right) = C_{1,1}^{2r-4}p_1^{2r-4}\left(x_{i-\frac{1}{2}}\right) + C_{1,2}^{2r-4}p_2^{2r-4}\left(x_{i-\frac{1}{2}}\right),$$

$$p_2^{2r-3}\left(x_{i-\frac{1}{2}}\right) = C_{2,2}^{2r-4}p_2^{2r-4}\left(x_{i-\frac{1}{2}}\right) + C_{2,3}^{2r-4}p_3^{2r-4}\left(x_{i-\frac{1}{2}}\right),$$

and so on, until the polynomials of degree $r + 1$ are reached,

$$p_l^{r+1}\left(x_{i-\frac{1}{2}}\right) = C_{l,l}^r p_l^r\left(x_{i-\frac{1}{2}}\right) + C_{l,l+1}^r p_{l+1}^r\left(x_{i-\frac{1}{2}}\right), \quad l = 0, \ldots, r - 2.$$

Thus, combining these equations,

$$\begin{aligned}
(30) \qquad p_0^{2r-1}(x_{i-\frac{1}{2}}) &= \sum_{j_0=0}^{1} C_{0,j_0}^{2r-2} p_{j_0}^{2r-2}\left(x_{i-\frac{1}{2}}\right) \\
&= \sum_{j_0=0}^{1} C_{0,j_0}^{2r-2}\left(\sum_{j_1=j_0}^{j_0+1} C_{j_0,j_1}^{2r-3} p_{j_1}^{2r-3}\left(x_{i-\frac{1}{2}}\right)\right) \\
&= \sum_{j_0=0}^{1} C_{0,j_0}^{2r-2}\left(\sum_{j_1=j_0}^{j_0+1} C_{j_0,j_1}^{2r-3}\left(\sum_{j_2=j_1}^{j_1+1} C_{j_1,j_2}^{2r-4} p_{j_2}^{2r-4}\left(x_{i-\frac{1}{2}}\right)\right)\right) \\
&= \sum_{j_0=0}^{1} C_{0,j_0}^{2r-2}\left(\sum_{j_1=j_0}^{j_0+1} C_{j_0,j_1}^{2r-3}\left(\ldots\left(\sum_{j_{r-2}=j_{r-3}}^{j_{r-3}+1} C_{j_{r-3},j_{r-2}}^{r+1} \right.\right.\right. \\
&\qquad \left.\left.\left. \times \left(\sum_{j_{r-1}=j_{r-2}}^{j_{r-2}+1} C_{j_{r-2},j_{r-1}}^{r} p_{j_{r-1}}^{r}\left(x_{i-\frac{1}{2}}\right)\right)\right)\ldots\right)\right).
\end{aligned}$$

In Figure 1 this process is shown for any r. It can be observed that the diagram shows a tree structure where from each node C_{k,k_1}^l, with $k_1 = k$ or $k_1 = k + 1$, we obtain two subnodes of the form C_{k_1,k_2}^{l-1} with $k_2 = k_1$ and $k_2 = k_1 + 1$, which allows an easy construction. The explicit values, C_{k,k_1}^l, are calculated using (29) of Lemma 3.1.

Therefore, it is easy to prove that the weights and the vector $\mathbf{C_k^{r+1}}$ with $0 \leq k \leq r - 2$ are
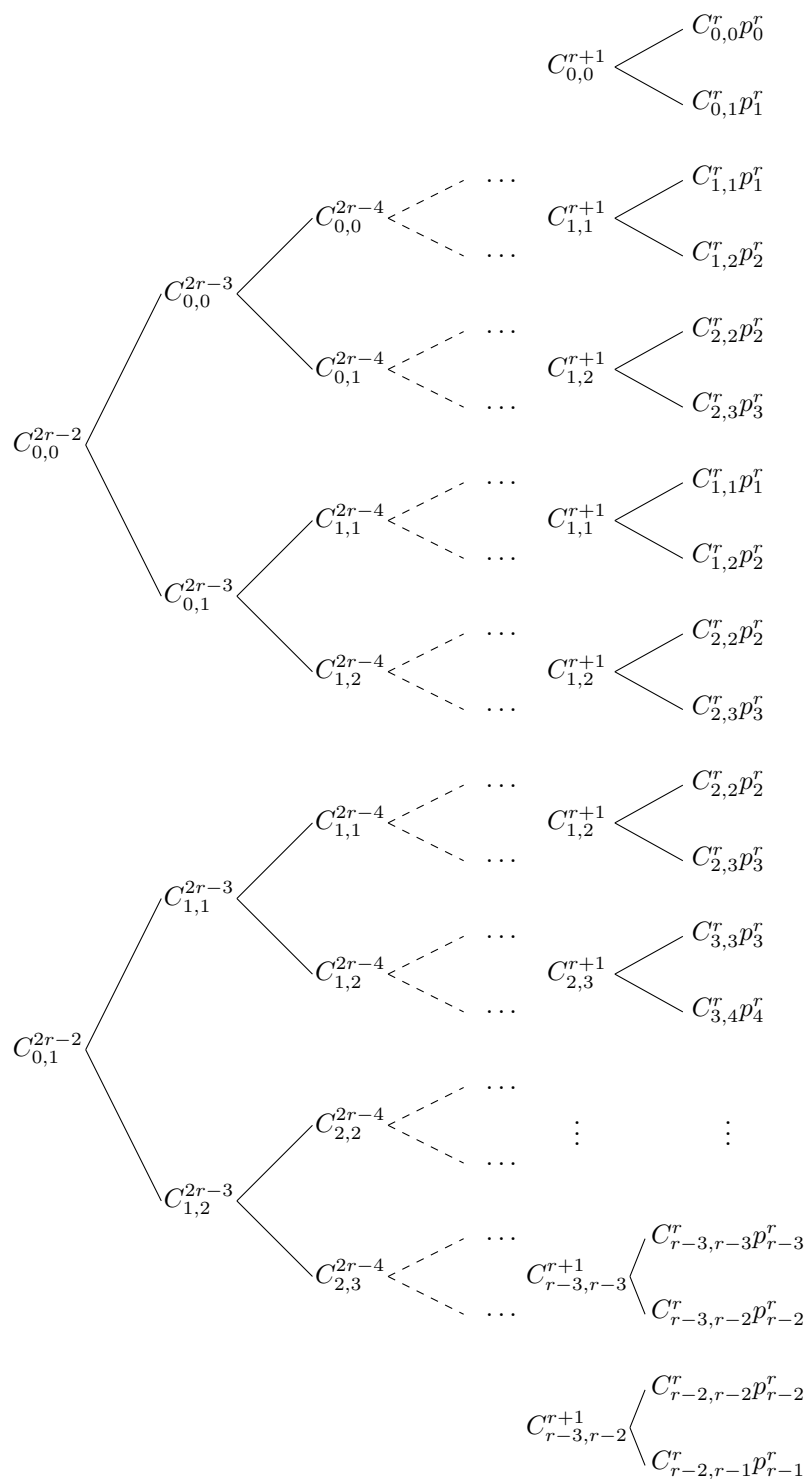
Fig. 1. *Diagram showing the structure of the optimal weights needed to obtain optimal order of accuracy.*

$$\mathbf{C_0^{r+1}} = (C_{0,0}^r, C_{0,1}^r, 0, 0, \ldots, 0) = \left(\frac{3}{2(r+1)}, \frac{2r-1}{2(r+1)}, 0, 0, \ldots, 0 \right),$$

$$\mathbf{C_1^{r+1}} = (0, C_{1,1}^r, C_{1,2}^r, 0, \ldots, 0) = \left(0, \frac{5}{2(r+1)}, \frac{2r-3}{2(r+1)}, 0, \ldots, 0 \right),$$

(31)
$$\vdots$$

$$\mathbf{C_{r-3}^{r+1}} = (0, \ldots, 0, C_{r-3,r-3}^r, C_{r-3,r-2}^r, 0) = \left(0, \ldots, 0, \frac{2r-3}{2(r+1)}, \frac{5}{2(r+1)}, 0 \right),$$

$$\mathbf{C_{r-2}^{r+1}} = (0, \ldots, 0, 0, C_{r-2,r-2}^r, C_{r-2,r-1}^r) = \left(0, \ldots, 0, 0, \frac{2r-1}{2(r+1)}, \frac{3}{2(r+1)} \right).$$

Hence, by construction, these weights satisfy

(32)
$$\sum_{j_0=0}^{1} C_{0,j_0}^{2r-2} \left(\sum_{j_1=j_0}^{j_0+1} C_{j_0,j_1}^{2r-3} \left(\sum_{j_2=j_1}^{j_1+1} C_{j_1,j_2}^{2r-4} \left(\cdots \left(\sum_{j_{r-2}=j_{r-3}}^{j_{r-3}+1} C_{j_{r-3},j_{r-2}}^{r+1} \mathbf{C_{j_{r-2}}^{r+1}} \right) \cdots \right) \right) \right)$$
$$= (\bar{C}_0^r, \bar{C}_1^r, \ldots, \bar{C}_{r-2}^r, \bar{C}_{r-1}^r) = \bar{\mathbf{C}}^\mathbf{r}.$$

In order to design the nonlinear weights, the values C_{k,k_1}^l are replaced in (32), for $l = r+1, \ldots, 2r-2$ and $0 \le k \le (2r-2) - l$, $k_1 = k, k+1$, by

(33)
$$\tilde{\omega}_{k,k_1}^l = \frac{\tilde{\alpha}_{k,k_1}^l}{\tilde{\alpha}_{k,k}^l + \tilde{\alpha}_{k,k+1}^l}, \quad k_1 = k, \ k+1,$$

$$\tilde{\alpha}_{k,k_1}^l = \frac{C_{k,k_1}^l}{(\epsilon + \tilde{I}_{k,k_1}^l)^t}, \quad k_1 = k, \ k+1,$$

where $\tilde{I}_{k,k_1}^l$ are the smoothness indicators introduced in [13] and will be analyzed in detail in section 4.1. Thus, the nonlinear weights are defined as

(34)

$$\tilde{\mathbf{C}}^\mathbf{r} = (\tilde{C}_0^r, \tilde{C}_1^r, \ldots, \tilde{C}_{r-2}^r, \tilde{C}_{r-1}^r)$$
$$= \sum_{j_0=0}^{1} \tilde{\omega}_{0,j_0}^{2r-2} \left(\sum_{j_1=j_0}^{j_0+1} \tilde{\omega}_{j_0,j_1}^{2r-3} \left(\sum_{j_2=j_1}^{j_1+1} \tilde{\omega}_{j_1,j_2}^{2r-4} \left(\cdots \left(\sum_{j_{r-2}=j_{r-3}}^{j_{r-3}+1} \tilde{\omega}_{j_{r-3},j_{r-2}}^{r+1} \mathbf{C_{j_{r-2}}^{r+1}} \right) \cdots \right) \right) \right).$$

Finally, for these weights, the WENO algorithm described in section 1 is applied using the nonlinear optimal weights in (34), i.e., we compute

$$\tilde{\mathcal{I}}(x_{i-\frac{1}{2}}; f) = \sum_{k=0}^{r} \tilde{\omega}_k^r p_k^r \left(x_{i-\frac{1}{2}} \right)$$

with

(35)
$$\tilde{\omega}_k^r = \frac{\tilde{\alpha}_k^r}{\sum_{j=0}^{r-1} \tilde{\alpha}_j}, \quad \text{with} \quad \tilde{\alpha}_k^r = \frac{\tilde{C}_k^r}{(\epsilon + \tilde{I}_k^r)^t}, \quad k = 0, \ldots, r-1,$$

where again the $\tilde{I}_k^r$, $k = 0, \ldots, r$, are the smoothness indicators defined in [16, 13].

In order to clarify this construction, the case $r = 5$ is presented because $r = 3$ and $r = 4$ have already been displayed in the previous section.

3.1. The case $r = 5$. In order to construct the nonlinear weights for $r = 5$, first, the vectors $\mathbf{C_k^6}$ can be calculated with $k = 0, 1, 2, 3$, thus

(36)
$$\mathbf{C_0^6} = \left(C_{0,0}^5, C_{0,1}^5, 0, 0, 0\right) = \left(\frac{1}{4}, \frac{3}{4}, 0, 0, 0\right), \quad \mathbf{C_1^6} = \left(0, C_{1,1}^5, C_{1,2}^5, 0, 0\right) = \left(0, \frac{5}{12}, \frac{7}{12}, 0, 0\right),$$
$$\mathbf{C_2^6} = \left(0, 0, C_{2,2}^5, C_{2,3}^5, 0\right) = \left(0, 0, \frac{7}{12}, \frac{5}{12}, 0\right), \quad \mathbf{C_3^6} = \left(0, 0, 0, C_{3,3}^5, C_{3,4}^5\right) = \left(0, 0, 0, \frac{3}{4}, \frac{1}{4}\right).$$

Second, the expressions of the following vectors can be obtained:

(37)
$$\tilde{\omega}_{0,0}^6 = \frac{\tilde{\alpha}_{0,0}^6}{\tilde{\alpha}_{0,0}^6 + \tilde{\alpha}_{0,1}^6}, \quad \tilde{\omega}_{0,1}^6 = \frac{\tilde{\alpha}_{0,1}^6}{\tilde{\alpha}_{0,0}^6 + \tilde{\alpha}_{0,1}^6}, \quad \tilde{\omega}_{1,1}^6 = \frac{\tilde{\alpha}_{1,1}^6}{\tilde{\alpha}_{1,1}^6 + \tilde{\alpha}_{1,2}^6}, \quad \tilde{\omega}_{1,2}^6 = \frac{\tilde{\alpha}_{1,2}^6}{\tilde{\alpha}_{1,1}^6 + \tilde{\alpha}_{1,2}^6},$$
$$\tilde{\omega}_{2,2}^6 = \frac{\tilde{\alpha}_{2,2}^6}{\tilde{\alpha}_{2,2}^6 + \tilde{\alpha}_{2,3}^6}, \quad \tilde{\omega}_{2,3}^6 = \frac{\tilde{\alpha}_{2,3}^6}{\tilde{\alpha}_{2,2}^6 + \tilde{\alpha}_{2,3}^6},$$
$$\tilde{\omega}_{0,0}^7 = \frac{\tilde{\alpha}_{0,0}^7}{\tilde{\alpha}_{0,0}^7 + \tilde{\alpha}_{0,1}^7}, \quad \tilde{\omega}_{0,1}^7 = \frac{\tilde{\alpha}_{0,1}^7}{\tilde{\alpha}_{0,0}^7 + \tilde{\alpha}_{0,1}^7}, \quad \tilde{\omega}_{1,1}^7 = \frac{\tilde{\alpha}_{1,1}^7}{\tilde{\alpha}_{1,1}^7 + \tilde{\alpha}_{1,2}^7}, \quad \tilde{\omega}_{1,2}^7 = \frac{\tilde{\alpha}_{1,2}^7}{\tilde{\alpha}_{1,1}^7 + \tilde{\alpha}_{1,2}^7},$$
$$\tilde{\omega}_{0,0}^8 = \frac{\tilde{\alpha}_{0,0}^8}{\tilde{\alpha}_{0,0}^8 + \tilde{\alpha}_{0,1}^8}, \quad \tilde{\omega}_{0,1}^8 = \frac{\tilde{\alpha}_{0,1}^8}{\tilde{\alpha}_{0,0}^8 + \tilde{\alpha}_{0,1}^8}$$

with

(38)
$$\tilde{\alpha}_{0,0}^6 = \frac{C_{0,0}^6}{(\epsilon + \tilde{I}_{0,0}^6)^t}, \quad \tilde{\alpha}_{0,1}^6 = \frac{C_{0,1}^6}{(\epsilon + \tilde{I}_{0,1}^6)^t}, \quad \tilde{\alpha}_{1,1}^6 = \frac{C_{1,1}^6}{(\epsilon + \tilde{I}_{1,1}^6)^t}, \quad \tilde{\alpha}_{1,2}^6 = \frac{C_{1,2}^6}{(\epsilon + \tilde{I}_{1,2}^6)^t},$$
$$\tilde{\alpha}_{2,2}^6 = \frac{C_{2,2}^6}{(\epsilon + \tilde{I}_{2,2}^6)^t}, \quad \tilde{\alpha}_{2,3}^6 = \frac{C_{2,3}^6}{(\epsilon + \tilde{I}_{2,3}^6)^t},$$
$$\tilde{\alpha}_{0,0}^6 = \frac{5/14}{(\epsilon + \tilde{I}_{0,0}^6)^t}, \quad \tilde{\alpha}_{0,1}^6 = \frac{9/14}{(\epsilon + \tilde{I}_{0,1}^6)^t}, \quad \tilde{\alpha}_{1,1}^6 = \frac{1/2}{(\epsilon + \tilde{I}_{1,1}^6)^t}, \quad \tilde{\alpha}_{1,2}^6 = \frac{1/2}{(\epsilon + \tilde{I}_{1,2}^6)^t},$$
$$\tilde{\alpha}_{0,0}^6 = \frac{9/14}{(\epsilon + \tilde{I}_{2,2}^6)^t}, \quad \tilde{\alpha}_{0,1}^6 = \frac{5/14}{(\epsilon + \tilde{I}_{2,3}^6)^t},$$
$$\tilde{\alpha}_{0,0}^7 = \frac{C_{0,0}^7}{(\epsilon + \tilde{I}_{0,0}^7)^t}, \quad \tilde{\alpha}_{0,1}^7 = \frac{C_{0,1}^7}{(\epsilon + \tilde{I}_{0,1}^7)^t}, \quad \tilde{\alpha}_{1,1}^7 = \frac{C_{1,1}^7}{(\epsilon + \tilde{I}_{1,1}^7)^t}, \quad \tilde{\alpha}_{1,2}^7 = \frac{C_{1,2}^7}{(\epsilon + \tilde{I}_{1,2}^7)^t},$$
$$\tilde{\alpha}_{0,0}^7 = \frac{7/16}{(\epsilon + \tilde{I}_{0,0}^7)^t}, \quad \tilde{\alpha}_{0,1}^7 = \frac{9/16}{(\epsilon + \tilde{I}_{0,1}^7)^t}, \quad \tilde{\alpha}_{1,1}^7 = \frac{9/16}{(\epsilon + \tilde{I}_{1,1}^7)^t}, \quad \tilde{\alpha}_{1,2}^7 = \frac{7/16}{(\epsilon + \tilde{I}_{1,2}^7)^t},$$
$$\tilde{\alpha}_{0,0}^8 = \frac{C_{0,0}^8}{(\epsilon + \tilde{I}_{0,0}^8)^t}, \quad \tilde{\alpha}_{0,1}^8 = \frac{C_{0,1}^8}{(\epsilon + \tilde{I}_{0,1}^8)^t},$$
$$\tilde{\alpha}_{0,0}^8 = \frac{1/2}{(\epsilon + \tilde{I}_{0,0}^8)^t}, \quad \tilde{\alpha}_{0,1}^8 = \frac{1/2}{(\epsilon + \tilde{I}_{0,1}^8)^t},$$

where $\tilde{I}_{k,k_1}^l$, with $l = 6, 7, 8$, $k = 0, 1, 2$, and $k_1 = k, k + 1$, are the smoothness indicators that will be defined in section 4.1. All in all, we get the new nonlinear weights,

(39)
$$\tilde{\mathbf{C}}^5 = (\tilde{C}_0^5, \tilde{C}_1^5, \tilde{C}_2^5, \tilde{C}_3^5, \tilde{C}_3^5) = \tilde{\omega}_{0,0}^8 \left(\tilde{\omega}_{0,0}^7 \left(\tilde{\omega}_{0,0}^6 \mathbf{C_0^6} + \tilde{\omega}_{0,1}^6 \mathbf{C_1^6}\right) + \tilde{\omega}_{0,1}^7 \left(\tilde{\omega}_{1,1}^6 \mathbf{C_1^6} + \tilde{\omega}_{1,2}^6 \mathbf{C_2^6}\right)\right)$$
$$+ \tilde{\omega}_{0,1}^8 \left(\tilde{\omega}_{1,1}^7 \left(\tilde{\omega}_{1,1}^6 \mathbf{C_1^6} + \tilde{\omega}_{1,2}^6 \mathbf{C_{2,2}^6}\right) + \tilde{\omega}_{1,2}^7 \left(\tilde{\omega}_{2,2}^6 \mathbf{C_2^6} + \tilde{\omega}_{2,3}^6 \mathbf{C_3^6}\right)\right).$$

Now the classical WENO method can be applied using these weights as optimal weights. In the next section, the properties of the smoothness indicators used in the algorithm for any value of r are explained and proved.

4. Smoothness indicators of high order. This section presents the smoothness indicators chosen, which allow us to obtain optimal order of accuracy close to the discontinuities. The ones introduced in [16] are appropriate, as they work well for detecting kinks and jumps in the function if the data is discretized in the point values (1). They can be defined as

$$(40) \qquad \tilde{I}_k^r = \sum_{l=2}^{r} h^{2l-1} \int_{x_{i-1}}^{x_i} \left(\frac{d^l}{dx^l} p_k^r(x) \right)^2 dx, \quad k = 0, \ldots, r-1.$$

For $r = 2, 3$, these weights satisfy several properties that allow us to obtain the condition shown in (6) (see [16]). In this section these results are extended for any r. In [14] the proof of the following theorem is given. It is reproduced here for completeness.

THEOREM 4.1. *Let $0 \leq k \leq r-1$ and let p_k^r be the interpolator polynomial of f of degree $r \geq 3$ that uses the nodes of the stencil S_k^r; then at smooth zones, the smoothness indicator obtained through* (40) *satisfies*

$$\tilde{I}_k^r = \left(h^2 (p_k^r)'' \left(x_{i-\frac{1}{2}} \right) \right)^2 \cdot (1 + O(h^2)).$$

Proof. Let $0 \leq k \leq r-1$ and let p_k^r be the interpolator polynomial of f of degree $r \geq 3$ that uses the nodes of the stencil S_k^r. It is an r times continuously differentiable function in a neighborhood of the point $x_{i-\frac{1}{2}} = x_i - h/2$. Then, $(p_k^{(l)}(x))^2$ can be written using the Taylor expansion of $p_k(x)$ as

$$\left((p_k^r)^{(l)}(x) \right)^2 = \left((p_k^r)^{(l)} \left(x_{i-\frac{1}{2}} \right) + (p_k^r)^{(l+1)} \left(x_{i-\frac{1}{2}} \right) \left(x - x_{i-\frac{1}{2}} \right) + O\left(\left(x - x_{i-\frac{1}{2}} \right)^2 \right) \right)^2$$

$$= \left((p_k^r)^{(l)} \left(x_{i-\frac{1}{2}} \right) \right)^2 + \left((p_k^r)^{(l+1)} \left(x_{i-\frac{1}{2}} \right) \left(x - x_{i-\frac{1}{2}} \right) \right)^2$$

$$+ 2 p_k^{(l)} \left(x_{i-\frac{1}{2}} \right) (p_k^r)^{(l+1)} \left(x_{i-\frac{1}{2}} \right) \left(x - x_{i-\frac{1}{2}} \right)$$

$$+ 2 (p_k^r)^{(l)} \left(x_{i-\frac{1}{2}} \right) (p_k^r)^{(l+2)} \left(x_{i-\frac{1}{2}} \right) \left(x - x_{i-\frac{1}{2}} \right)^2 + O\left(\left(x - x_{i-\frac{1}{2}} \right)^3 \right).$$

Integrating the previous expression between x_{i-1} and x_i, replacing in (40), and simplifying, the result is obtained, as for $l > 2$ all the terms of the summation have a size smaller than or equal to $O(h^6)$,

$$\tilde{I}_k^r = \sum_{l=2}^{r} h^{2l-1} \int_{x_{i-1}}^{x_i} \left((p_k^r)^{(l)}(x) \right)^2 dx = \sum_{l=2}^{r} \left(h^l (p_k^r)^{(l)} \left(x_{i-\frac{1}{2}} \right) \right)^2 \cdot (1 + O(h^2))$$

$$= \left(h^2 (p_k^r)'' \left(x_{i-\frac{1}{2}} \right) \right)^2 \cdot (1 + O(h^2)). \qquad \square$$

The following proposition is proved in [16].

PROPOSITION 4.2. *Let be $0 \leq k < r$, $1 \leq t$, and $\tilde{\omega}_k^r$ be the nonlinear weights defined in* (35). *Then,*

$$\tilde{\omega}_k^r = O(1) \quad \text{if } f \text{ is smooth in } S_k^r,$$
$$\tilde{\omega}_k^r = O(h^{2mt}) \quad \text{if } f \text{ is not smooth in } S_k^r$$

with $m = 2$ if the discontinuity is in the function and $m = 1$ if the discontinuity is in the first derivative.

In what follows, the explicit form of $\tilde{I}_k^r$ with $k = 0, \ldots, r - 1$ for $r = 3, 4$ is given. The second order undivided differences are noted by $\delta_i^2 = f_i - 2 f_{i+1} + f_{i+2}$, $\delta_i^3 = \delta_{i+1}^2 - \delta_i^2$, and $\delta_i^4 = \delta_{i+1}^3 - \delta_i^3$. Taking into account the previous notation for the differences, the smoothness indicators in (40) for $r = 3$ are

$$(41) \qquad \begin{aligned} \tilde{I}_0^3 &= \frac{10}{3} \left(\delta_{i-3}^3 + \frac{9}{20} \delta_{i-3}^2 \right)^2 + \frac{13}{40} (\delta_{i-3}^2)^2, \\ \tilde{I}_1^3 &= \frac{4}{3} \left(\delta_{i-2}^3 + \frac{3}{8} \delta_{i-2}^2 \right)^2 + \frac{13}{16} (\delta_{i-2}^2)^2, \\ \tilde{I}_2^3 &= \frac{4}{3} \left(\delta_{i-1}^3 - \frac{3}{8} \delta_{i-1}^2 \right)^2 + \frac{13}{16} (\delta_{i-1}^2)^2. \end{aligned}$$

For $r = 4$ they can be written as

$$\begin{aligned}
\tilde{I}_0^4 &= \frac{22}{3} \left(\frac{81}{88} \delta_{i-4}^4 + \delta_{i-4}^3 + \frac{15}{44} \delta_{i-4}^2 \right)^2 + \frac{2107}{240} \left(\delta_{i-4}^4 + \frac{440}{2107} \delta_{i-4}^2 \right)^2 \\
&\quad - \frac{3}{88} \left(\frac{27}{2} \delta_{i-4}^4 + 5 \delta_{i-4}^2 \right)^2 + \frac{3901}{6321} (\delta_{i-4}^2)^2, \\
\tilde{I}_1^4 &= \frac{10}{3} \left(\frac{19}{40} \delta_{i-3}^4 + \delta_{i-3}^3 + \frac{9}{20} \delta_{i-3}^2 \right)^2 + \frac{547}{240} \left(\delta_{i-3}^4 + \frac{80}{547} \delta_{i-3}^2 \right)^2 \\
&\quad - \frac{3}{40} \left(\frac{19}{6} \delta_{i-3}^4 + 3 \delta_{i-3}^2 \right)^2 + \frac{1561}{1641} (\delta_{i-3}^2)^2, \\
\tilde{I}_2^4 &= \frac{4}{3} \left(-\frac{1}{16} \delta_{i-2}^4 + \delta_{i-2}^3 + \frac{3}{8} \delta_{i-2}^2 \right)^2 + \frac{89}{80} \left(\delta_{i-2}^4 - \frac{40}{267} \delta_{i-2}^2 \right)^2 \\
&\quad - \frac{3}{16} \left(-\frac{1}{6} \delta_{i-2}^4 + \delta_{i-2}^2 \right)^2 + \frac{781}{801} (\delta_{i-2}^2)^2, \\
\tilde{I}_3^4 &= \frac{4}{3} \left(-\frac{15}{16} \delta_{i-1}^4 + \delta_{i-1}^3 - \frac{3}{8} \delta_{i-1}^2 \right)^2 + \frac{547}{240} \left(\delta_{i-1}^4 + \frac{80}{547} \delta_{i-1}^2 \right)^2 \\
&\quad - \frac{3}{16} \left(-\frac{5}{2} \delta_{i-1}^4 - \delta_{i-1}^2 \right)^2 + \frac{1561}{1641} (\delta_{i-1}^2)^2.
\end{aligned}$$

(42)

Once the smoothness indicators for the level r are defined, the rest of the indicators for each level can be constructed from $2r - 2$ to $r + 1$. Theorem 4.1 allows us to have a clearer vision about the behavior of the smoothness indicators. We can see that they get a value that is $O(h^4)$ at smooth zones. As they can be expressed in terms of differences, they get a value that is $O(1)$ when their stencil contains a discontinuity.

In [14], in order to reduce the computational cost of the calculation of smoothness indicators of high order through (40), it is proposed to use a function of the smoothness indicators implemented by the classical WENO algorithm. For $r = 3$ the smoothness indicators of five points were given by

$$(43) \qquad \begin{aligned} \tilde{I}_{0,0}^4 &= \tilde{I}_0^3 + \tilde{I}_1^3, \\ \tilde{I}_{0,1}^4 &= \tilde{I}_1^3 + \tilde{I}_2^3. \end{aligned}$$

These smoothness indicators provide optimal accuracy for $r = 3$ in the sense that the pattern of accuracy obtained close to a discontinuity is $\dots, O(h^6), O(h^5), O(h^4), O(1)$, $O(h^4), O(h^5), O(h^6), \dots$. For $r = 4$, the smoothness indicators of six and seven points $\tilde{I}_{0,0}^5, \tilde{I}_{0,1}^5, \tilde{I}_{1,2}^5, \tilde{I}_{0,0}^6, \tilde{I}_{0,1}^6$ were defined as

$$(44) \qquad \begin{aligned} \tilde{I}_{0,0}^5 &= \tilde{I}_0^4 + \tilde{I}_1^4, \quad \tilde{I}_{0,1}^5 = \tilde{I}_{0,1}^5 = \tilde{I}_1^4 + \tilde{I}_2^4, \quad \tilde{I}_{1,2}^5 = \tilde{I}_2^4 + \tilde{I}_3^4, \\ \tilde{I}_{0,0}^6 &= \tilde{I}_0^4 + \tilde{I}_1^4 + \tilde{I}_2^4, \quad \tilde{I}_{0,1}^6 = \tilde{I}_1^4 + \tilde{I}_2^4 + \tilde{I}_3^4. \end{aligned}$$

In this case, these smoothness indicators do not provide optimal accuracy, providing the typical pattern of accuracy close to the discontinuity $\dots, O(h^8), O(h^7), O(h^5)$, $O(h^5), O(1), O(h^5), O(h^5), O(h^7), O(h^8), \cdots$ instead of the optimal one $\dots, O(h^8)$, $O(h^7), O(h^6), O(h^5), O(1), O(h^5), O(h^6), O(h^7), O(h^8), \dots$. The reason is the following. Let's observe Figure 2, which represents the stencil of eight points considered for $r = 4$. This figure represents a discontinuity in the interval (x_{i+1}, x_{i+2}) (the case for the discontinuity in the interval (x_{i-3}, x_{i-2}) is symmetric). Let's now recall the expression of the interpolation proposed in [14] and reproduced in (26). The smoothness indicators $\tilde{I}_{0,0}^6$ and $\tilde{I}_{0,1}^6$ in (44) use the data placed at the positions $\{x_{i-4}, \dots, x_{i+2}\}$ and $\{x_{i-3}, \dots, x_{i+3}\}$, respectively. Looking at their expressions in (44), it is clear that the weights $\tilde{\omega}_{0,0}^6$ and $\tilde{\omega}_{0,1}^6$ in (25) are both affected by the discontinuity, so both of them will have $O(1)$ accuracy. For a good approximation of the case represented in Figure 2, $\tilde{\omega}_{0,0}^6 \approx 1$ and $\tilde{\omega}_{0,1}^6 \approx 0$ in order to keep the final weights close to the optimal ones. The problem would be solved if $\tilde{\omega}_{1,1}^5 \approx 0$ and $\tilde{\omega}_{1,2}^5 \approx 0$ but this is not possible, as the algorithm balances the weights in pairs of two; thus, if one is close to zero the other one must be close to one. The problem is solved in this case if the smoothness indicators are selected in pairs as

$$(45) \qquad \begin{aligned} \tilde{I}_{0,0}^6 &= \tilde{I}_0^4, \quad \tilde{I}_{0,1}^6 = \tilde{I}_3^4, \\ \tilde{I}_{0,0}^5 &= \tilde{I}_0^4, \quad \tilde{I}_{0,1}^5 = \tilde{I}_2^4, \\ \tilde{I}_{1,1}^5 &= \tilde{I}_1^4, \quad \tilde{I}_{1,2}^5 = \tilde{I}_3^4. \end{aligned}$$

Now it is clear that $\tilde{\omega}_{0,0}^6$ *watches* the discontinuity and it gets a value $\tilde{\omega}_{0,0}^6 \approx 1$ while $\tilde{\omega}_{0,1}^6 \approx 0$, cleaning the garbage introduced if (44) is used and similarly for $\tilde{\omega}_{0,1}^5$ with $k = 0, 1, k_1 = k + 1$. With this strategy only the smoothness indicators of degree r are computed, which are the ones used by the classical WENO algorithm, improving the computational efficiency.

In the following subsection a general formula is given for computing the smoothness indicator for any r.

4.1. General smoothness indicators. In this subsection a general formula is provided in order to obtain any smoothness indicator I_{k,k_1}^l in terms of the clas-

FIG. 2. *Representation of the values considered in the stencil and a discontinuity placed in the interval* $[x_{i+1}, x_{i+2}]$.

sical WENO smoothness indicators $\tilde{I}_k^r$ for r. We follow the same construction presented previously in this section. The different weights are defined using the following formulas.

DEFINITION 4.1. *Let be $l = r + 1, \ldots, 2r - 2$, and $\tilde{I}_k^r$, with $k = 0, \ldots, r - 1$ the smoothness indicators showed in* (40); *then the smoothness indicators at level l can be defined as*

$$
\begin{aligned}
\tilde{I}_{k,k}^l &= \tilde{I}_k^r, \quad k = 0, \ldots, (2r - 2) - l, \\
\tilde{I}_{k,k+1}^l &= \tilde{I}_{l-(r-1)+k}^r, \quad k = 0, \ldots, (2r - 2) - l.
\end{aligned}
\tag{46}
$$

The idea is to detect in what part of the tree diagram the discontinuity is placed and to force this branch to be automatically discarded through the values of the smoothness indicators and, consequently, the weights. Then continue with the following subbranch and again force the automatic discarding of this branch if the stencil contains a discontinuity. This process is repeated in each pass until only one branch free of discontinuities is found.

The smoothness indicators for $r = 3$ and $r = 4$ already have been described. For $r = 5$, using (46),

$$
\begin{aligned}
\tilde{I}_{0,0}^8 &= \tilde{I}_0^5, \quad \tilde{I}_{0,1}^8 = \tilde{I}_4^5, \\
\tilde{I}_{0,0}^7 &= \tilde{I}_0^5, \quad \tilde{I}_{0,1}^7 = \tilde{I}_3^5, \quad \tilde{I}_{1,1}^7 = \tilde{I}_1^5, \quad \tilde{I}_{1,2}^7 = \tilde{I}_4^5, \\
\tilde{I}_{0,0}^6 &= \tilde{I}_0^5, \quad \tilde{I}_{0,1}^6 = \tilde{I}_2^5, \quad \tilde{I}_{1,1}^6 = \tilde{I}_1^5, \quad \tilde{I}_{1,2}^6 = \tilde{I}_3^5.
\end{aligned}
\tag{47}
$$

Finally, we prove the following important results that will be used in the next section in order to analyze the accuracy of the new method.

LEMMA 4.3. *Let be $0 \le k, k_1 \le r - 2$, and $\tilde{I}_n^r$, $n = k, k_1$, be smoothness indicators of f on the stencil $S_n^r = \{x_{i+n-r}, \ldots, x_{i+n}\}$. If $f \in C^r([x_{i+n-r}, x_{i+n}])$, then*

$$
\tilde{I}_k^r - \tilde{I}_{k_1}^r = O(h^{r+3}),
$$

Proof. Let $p_k^r, p_{k_1}^r$ be the two interpolating polynomials of f of degree $r \ge 3$ at nodes in the stencil S_n^r, $n = k, k_1$, at a distance $O(h)$. Then if $l \ge 2$, the sketch of the proof presented in [4] can be followed, and thus from $(f^{(l)}) - (p_n^r)^{(l)} = O(h^{r+1-l})$, we get

$$
\begin{aligned}
\left(f^{(l)}\right)^2 - \left((p_n^r)^{(l)}\right)^2 &= -\left(\left(f^{(l)} - (p_n^r)^{(l)}\right)^2 + 2\left((p_n^r)^{(l)} - f^{(l)}\right) f^{(l)}\right) \\
&= \left(O\left(h^{r+1-l}\right)\right)^2 + (O\left(h^{r+1-l}\right))O(1) \\
&= O\left(h^{r+1-l}\right),
\end{aligned}
\tag{48}
$$

and replacing in (40), we obtain

$$
\begin{aligned}
\left| \tilde{I}_n^r - \sum_{l=2}^r h^{2l-1} \int_{x_{i-1}}^{x_i} \left(f^{(l)}(x)\right)^2 dx \right| &\le \left| \sum_{l=2}^r h^{2l-1} \int_{x_{i-1}}^{x_i} \left((p_n^r)^{(l)}(x)\right)^2 - \left(f^{(l)}(x)\right)^2 dx \right| \\
&= \sum_{l=2}^r h^{2l} O\left(h^{r+1-l}\right) \\
&= O(h^{r+3}).
\end{aligned}
$$

Finally,

(49)
$$\left| \tilde{I}_k^r - \tilde{I}_{k_1}^r \right| \le \left| \tilde{I}_k^r - \sum_{l=2}^{r} h^{2l-1} \int_{x_{i-1}}^{x_i} \left(f^{(l)}(x) \right)^2 dx \right| + \left| \tilde{I}_{k+1}^r - \sum_{l=2}^{r} h^{2l-1} \int_{x_{i-1}}^{x_i} \left(f^{(l)}(x) \right)^2 dx \right|$$
$$= O(h^{r+3}). \qquad \square$$

PROPOSITION 4.4. *Let be* $r + 1 \le l \le 2r - 2$, $0 \le k \le (2r - 2) - l$ *and* $\tilde{I}_{k,k}^l$ *and* $\tilde{I}_{k,k+1}^l$ *be smoothness indicators defined in Definition 4.1, which can be expressed, following Theorem 4.1, through Taylor expansion as* $\tilde{I}_{k,k}^l = (h^2 p''(x_{i-\frac{1}{2}}))^2(1 + O(h^2))$ *if the stencil is smooth,* $\tilde{I}_{k,k}^l = O(1)$ *if the stencil is affected by a discontinuity in the function, and* $\tilde{I}_{k,k}^l = O(h)$ *if the stencil is affected by a discontinuity in the first derivative. In this case, any weights expressed as*

(50)
$$\tilde{\omega}_{k,k}^l = \frac{\tilde{\alpha}_{k,k}^l}{\tilde{\alpha}_{k,k}^l + \tilde{\alpha}_{k,k+1}^l}, \quad \tilde{\omega}_{k,k+1}^l = \frac{\tilde{\alpha}_{k,k+1}^l}{\tilde{\alpha}_{k,k}^l + \tilde{\alpha}_{k,k+1}^l}$$

with

(51)
$$\tilde{\alpha}_{k,k}^l = \frac{C_{k,k}^l}{(\epsilon + \tilde{I}_{k,k}^l)^t}, \quad \tilde{\alpha}_{k,k+1}^l = \frac{C_{k,k+1}^l}{(\epsilon + \tilde{I}_{k,k+1}^l)^t}$$

with $C_{k,k}^l + C_{k,k+1}^l = 1$ *will fall under one of the following cases:*
  1. *If neither* $\tilde{I}_{k,k}^l$ *nor* $\tilde{I}_{k,k+1}^l$ *is affected by a discontinuity, then* $\tilde{\omega}_{k,k}^l = C_{k,k}^l + O(h^{r-1})$ *and* $\tilde{\omega}_{k,k+1}^l = C_{k,k+1}^l + O(h^{r-1})$.
  2. *If* $\tilde{I}_{k,k+1}^l$ *is affected by a singularity, then* $\tilde{\omega}_{k,k}^l = 1 + O(h^{2mt})$ *and* $\tilde{\omega}_{k,k+1}^l = O(h^{2mt})$.
  3. *Symmetrically, if* $\tilde{I}_{k,k}^l$ *is affected by a singularity, then* $\tilde{\omega}_{k,k+1}^l = 1 + O(h^{2mt})$ *and* $\tilde{\omega}_{k,k}^l = O(h^{2mt})$.
  4. *If* $\tilde{I}_{k,k}^l$ *and* $\tilde{I}_{k,k+1}^l$ *are affected by a singularity, then* $\tilde{\omega}_{k,k}^l = O(1)$ *and* $\tilde{\omega}_{k,k+1}^l = O(1)$.
Here $m = 2$ *if the discontinuity is in the function and* $m = 1$ *if the discontinuity is in the first derivative.*

Proof. The ideas presented in [4] can be followed. Let $r + 1 \le l \le (2r - 2)$ and $0 \le k \le (2r - 2) - l$; by Definition 4.1,

(52)
$$\tilde{I}_{k,k}^l = \tilde{I}_k^r, \quad \tilde{I}_{k,k+1}^l = \tilde{I}_{l-(r-1)+k}^r = \tilde{I}_{k_1}^r,$$

where $k_1 = l - (r - 1) + k$, doing algebraic manipulations,

$$\frac{\frac{1}{(\epsilon + \tilde{I}_k^r)^t} + \frac{1}{(\epsilon + \tilde{I}_{k_1}^r)^t}}{\frac{1}{(\epsilon + \tilde{I}_{k_1}^r)^t}} = \frac{\tilde{I}_{k_1}^r - \tilde{I}_k^r}{\epsilon + \tilde{I}_k^r} \sum_{j=0}^{t-1} \left(\frac{\epsilon + \tilde{I}_{k_1}^r}{\epsilon + \tilde{I}_k^r} \right)^j,$$

then, using Lemma 4.3, the previous equality transforms into

(53)
$$\frac{1}{(\epsilon + \tilde{I}_k^r)^t} = \frac{1 + O(h^{r-1})}{(\epsilon + \tilde{I}_{k_1}^r)^t}.$$

If there is no singularity affecting $\tilde{I}^r_{k,k} = \tilde{I}^r_k$ or $\tilde{I}^r_{k,k+1} = \tilde{I}^r_{k_1}$ then, using (53),

(54)
$$\tilde{\omega}^l_{k,k} = \frac{\frac{C^l_{k,k}}{(\epsilon+\tilde{I}^l_{k,k})^t}}{\frac{C^l_{k,k}}{(\epsilon+\tilde{I}^l_{k,k})^t} + \frac{C^l_{k,k+1}}{(\epsilon+\tilde{I}^l_{k,k+1})^t}} = \frac{\frac{C^l_{k,k}}{(\epsilon+\tilde{I}^r_k)^t}}{\frac{C^l_{k,k}}{(\epsilon+\tilde{I}^r_k)^t} + \frac{\tilde{C}^l_{k,k+1}}{(\epsilon+\tilde{I}^r_{k_1})^t}} = \frac{\frac{C^l_{k,k}(1+O(h^{r-1}))}{(\epsilon+\tilde{I}^r_{k_1})^t}}{\frac{C^l_{k,k}(1+O(h^{r-1}))}{(\epsilon+\tilde{I}^r_{k_1})^t} + \frac{C^l_{k,k+1}}{(\epsilon+\tilde{I}^r_{k_1})^t}}$$
$$= \frac{C^l_{k,k}(1+O(h^{r-1}))}{C^l_{k,k}(1+O(h^{r-1})) + C^l_{k,k+1}}$$
$$= C^l_{k,k} + O(h^{r-1}).$$

Analogously,
$$\tilde{\omega}^l_{k,k+1} = C^l_{k,k+1} + O(h^{r-1}).$$

If, following Theorem 4.1, $\tilde{I}^l_{k,k} = K(1+O(h^2))$ if the stencil is smooth and $\tilde{I}^l_{k,k} = O(1)$ if the stencil is affected by a discontinuity and considering that ϵ is small enough, then

1. if the stencil contains a singularity that only affects the smoothness indicator $\tilde{I}^l_{k,k+1}$, then $\tilde{I}^l_{k,k} = (h^2 p''(x_{i-\frac{1}{2}}))^2(1 + O(h^2)) = O(h^{2m})$ with $m = 2$ if the discontinuity is in the function and $m = 1$ if the discontinuity is in the first derivative, and $\tilde{I}^l_{k,k+1} = O(1)$; then,

(55)
$$\tilde{\omega}^l_{k,k} = \frac{C^l_{k,k}(\epsilon + \tilde{I}^l_{k,k+1})^t}{C^l_{k,k}(\epsilon+\tilde{I}^l_{k,k+1})^t + C^l_{k,k+1}(\epsilon + \tilde{I}^l_{k,k})^t} = \frac{C^l_{k,k}(\epsilon+\tilde{I}^l_{k,k+1})^t}{C^l_{k,k}(\epsilon + \tilde{I}^l_{k,k+1})^t + O(h^{2mt})}$$
$$= \frac{C^l_{k,k}(\epsilon + \tilde{I}^l_{k,k+1})^t}{C^l_{k,k}(\epsilon + \tilde{I}^l_{k,k+1})^t} \frac{1}{1 + \frac{O(h^{2mt})}{C^l_{k,k}(\epsilon+\tilde{I}^l_{k,k+1})^t}}$$
$$= 1 + O(h^{2mt}),$$
$$\tilde{\omega}^l_{k,k+1} = \frac{C^l_{k,k+1}(\epsilon + \tilde{I}^l_{k,k})^t}{C^l_{k,k}(\epsilon+\tilde{I}^l_{k,k+1})^t + C^l_{k,k+1}(\epsilon + \tilde{I}^l_{k,k})^t} = \frac{O(h^{2mt})}{O(1)+O(h^{2mt})} = O(h^{2mt}).$$

2. the case when the stencil contains a singularity that only affects the smoothness indicator $I_{k,k}$ can be obtained by symmetry;

3. if $\tilde{I}^l_{k,k}$ and $\tilde{I}^l_{k,k+1}$ are affected by a singularity, then

(56)
$$\tilde{\omega}^l_{k,k} = \frac{C^l_{k,k}(\epsilon + \tilde{I}^l_{k,k+1})^t}{C^l_{k,k}(\epsilon+\tilde{I}^l_{k,k+1})^t + C^l_{k,k+1}(\epsilon+\tilde{I}^l_{k,k})^t} = \frac{C^l_{k,k}(\epsilon+\tilde{I}^l_{k,k+1})^t}{C^l_{k,k}(\epsilon + \tilde{I}^l_{k,k+1})^t + O(h^{2mt})}$$
$$= \frac{C^l_{k,k}(\epsilon + \tilde{I}^n_{k,k+1})^t}{C^n_{k,k}(\epsilon + \tilde{I}^l_{k,k+1})^t} \frac{1}{1 + \frac{O(h^{2mt})}{O(h^{2mt})}} = O(1),$$
$$\tilde{\omega}^l_{k,k+1} = \frac{C^l_{k,k+1}(\epsilon + \tilde{I}^l_{k,k})^t}{C^l_{k,k}(\epsilon + \tilde{I}^l_{k,k+1})^t + C^n_{k,k+1}(\epsilon + \tilde{I}^l_{k,k})^t} = O(1). \qquad \square$$

5. Analysis of the accuracy. Let us try to analyze now the accuracy of each individual dyadic WENO algorithm that we perform at every step of the new construction. In general, to prove the accuracy of this algorithm three steps are needed:

1. Obtaining the value that the nonlinear optimal weights get for each position of the discontinuity.

2. Checking the error obtained between the weights of the classical WENO (that is performed at the last step) obtained using the nonlinear optimal weights and the weights that provide optimal accuracy.

3. Checking the accuracy obtained by classical WENO interpolation.

5.1. Analysis of the accuracy for any r. This section presents a general study of the accuracy of the new algorithm using the formulas described in section 3. Therefore, the weights are given by

$$(\tilde{C}_0^r, \tilde{C}_1^r, \ldots, \tilde{C}_{r-2}^r, \tilde{C}_{r-1}^r)$$
$$= \sum_{j_0=0}^{1} \tilde{\omega}_{0,j_0}^{2r-2} \left(\sum_{j_1=j_0}^{j_0+1} \tilde{\omega}_{j_0,j_1}^{2r-3} \left(\sum_{j_2=j_1}^{j_1+1} \tilde{\omega}_{j_1,j_2}^{2r-4} \left(\ldots \left(\sum_{j_{r-2}=j_{r-3}}^{j_{r-3}+1} \tilde{\omega}_{j_{r-3},j_{r-2}}^{r+1} \mathbf{C_{j_{r-2}}^{r+1}} \right) \ldots \right) \right) \right),$$

where the values $\tilde{\omega}_{k,k_1}^l$ with $l = r+1, \ldots, 2r-2$; $0 \le k \le (2r-2)-l$; $k_1 = k+1$ and $\mathbf{C_k^{r+1}}$ being $0 \le k \le r-2$, are defined in (33) and (31). The coordinates of the vector $(\tilde{\omega}_0^r, \ldots, \tilde{\omega}_{r-1}^r)$ have been defined in (35), i.e.,

(57)
$$\tilde{\omega}_k^r = \frac{\tilde{\alpha}_k^r}{\sum_{s=0}^{r-1} \tilde{\alpha}_s^r}, \quad k = 0, \ldots, r-1,$$
$$\tilde{\alpha}_k^r = \frac{\tilde{C}_k^r}{(\epsilon + \tilde{I}_k^r)^t}, \quad k = 0, \ldots, r-1.$$

The different possibilities can be analyzed.

- First, we suppose that any discontinuity does not cross the stencil $\{x_{i-r}, \ldots, x_{i+r-1}\}$; then by Proposition 4.4, we get for all $l = r+1, \ldots, 2r-2$, $0 \le k \le (2r-2)-l$, and $k_1 = k+1$ that

$$\tilde{\omega}_{k,k_1}^l = \tilde{C}_{k,k_1}^l + O(h^{r-1}).$$

Then, by construction of the optimal weights, (30),

$$(\tilde{\omega}_0^r, \ldots, \tilde{\omega}_{r-1}^r) = (\tilde{C}_0^r, \ldots, \tilde{C}_{r-1}^r) + O(h^{r-1})$$
$$= \sum_{j_0=0}^{1} \tilde{\omega}_{0,j_0}^{2r-2} \left(\sum_{j_1=j_0}^{j_0+1} \tilde{\omega}_{j_0,j_1}^{2r-3} \left(\sum_{j_2=j_1}^{j_1+1} \tilde{\omega}_{j_1,j_2}^{2r-4} \left(\ldots \left(\sum_{j_{r-2}=j_{r-3}}^{j_{r-3}+1} \right. \right. \right. \right.$$
$$\times \tilde{\omega}_{j_{r-3},j_{r-2}}^{r+1} \mathbf{C_{j_{r-2}}^{r+1}} \left. \left. \left. \left. \ldots \right) \right) \right) \right) + O(h^{r-1})$$
$$= \sum_{j_0=0}^{1} C_{0,j_0}^{2r-2} \left(\sum_{j_1=j_0}^{j_0+1} C_{j_0,j_1}^{2r-3} \left(\sum_{j_2=j_1}^{j_1+1} C_{j_1,j_2}^{2r-4} \left(\ldots \left(\sum_{j_{r-2}=j_{r-3}}^{j_{r-3}+1} \right. \right. \right. \right.$$
$$\times C_{j_{r-3},j_{r-2}}^{r+1} \mathbf{C_{j_{r-2}}^{r+1}} \left. \left. \left. \left. \ldots \right) \right) \right) \right) + O(h^{r-1})$$
$$= (\bar{C}_0^r, \ldots, \bar{C}_{r-1}^r) + O(h^{r-1}).$$

- If there exists a discontinuity at $[x_{i-1}, x_i]$ by Proposition 4.4, for all $l = r+1, \ldots, 2r-2$, $0 \le k \le (2r-2)-l$, and $k_1 = k+1$ we get

$$\tilde{\omega}_{k,k_1}^l = O(1).$$

- Using symmetry arguments, we only need to analyze the case when there exists an isolated discontinuity at an interval $[x_{i-1+l_0}, x_{i+l_0}]$, $l_0 = 1, \ldots, r-1$ (analogously, the equivalent symmetric results for $[x_{i-r+l_0}, x_{i-r+l_0+1}]$, $l_0 = 0, \ldots, r-2$ can be obtained). In order to study these cases, the following results are shown.

LEMMA 5.1. *Let $\tilde{\omega}_k^r$, $k = 0, \ldots, r-1$, be the nonlinear weights defined in* (35). *If there exists $0 \le l_0 \le r-1$ such that $I_{l_0}^r$ is affected by a discontinuity and*

$$(\tilde{C}_0^r, \ldots, \tilde{C}_{r-1}^r) = (C_0^r + O(h^s), \ldots, C_{l_0-1}^r + O(h^s), O(h^{2mt}), \ldots, O(h^{2mt}))$$

with $\sum_{k=0}^{l_0-1} C_k^r = 1$, $1 \le s \le 2mt$, $m = 2$ if the discontinuity is in the function and $m = 1$ if the discontinuity is in the first derivative, then

$$\tilde{\omega}_k^r = C_k^r + O(h^s), \quad 0 \le k < l_0,$$
$$\tilde{\omega}_k^r = O(h^{2mt}), \quad l_0 \le k \le r-1.$$

Proof. This is a direct consequence of the fact that $\sum_{k=0}^{l_0-1} C_k^r = 1$. □

LEMMA 5.2. *Let be $0 < l_0 \le r-1$. If there exists a discontinuity at $[x_{i+l_0-1}, x_{i+l_0}]$, then for all $l_0 + (r-1) \le l \le 2r-2$ the nonlinear weights defined in* (33) *satisfy*

(58) $$\tilde{\omega}_{0,0}^l = 1 + O(h^{2mt}), \quad \tilde{\omega}_{0,1}^l = O(h^{2mt}),$$

where $m = 2$ if the discontinuity is in the function and $m = 1$ if the discontinuity is in the first derivative.

Proof. It is clear that as $l_0 > 0$, then the smoothness indicator $\tilde{I}_0^r$ is not affected by the discontinuity. However, if $l_0 + (r-1) \le l \le 2r-2$, then

$$l - (r-1) - r < 0 < l_0 = l_0 + (r-1) - (r-1) \le l - (r-1).$$

Thus, the discontinuity crosses the stencil used to calculate $\tilde{I}_{l-(r-1)}^r$ and then, by the definition of the smoothness indicators in (46), we get

$$\tilde{I}_{0,0}^l = \tilde{I}_0^r, \quad \tilde{I}_{0,1}^l = \tilde{I}_{l-(r-1)}^r,$$

and by Proposition 4.4 the result is obtained, i.e.,

$$\tilde{\omega}_{0,0}^l = 1 + O(h^{2mt}), \quad \tilde{\omega}_{0,1}^l = O(h^{2mt}). \qquad \square$$

LEMMA 5.3. *Let $0 < l_0 \le r-1$. If there exists a discontinuity at $[x_{i+l_0-1}, x_{i+l_0}]$, then for all $r+1 \le l \le l_0 + (r-2)$ the nonlinear weights defined in* (33) *satisfy*

(59)
$$\tilde{\omega}_{k,k}^l = C_{k,k}^l + O(h^{r-1}), \quad \tilde{\omega}_{k,k+1}^l = C_{k,k+1}^l + O(h^{r-1}), \quad 0 \le k \le l_0 + (r-2) - l,$$

where C_{k,k_1}^l with $k_1 = k$, $k+1$ defined in (29).

Proof. In order to prove this lemma, we only have to analyze if the discontinuity crosses the stencils used to calculate $\tilde{I}_k^r$ and $\tilde{I}_{l-(r-1)+k}^r$. In the first case, the stencil is $\{x_{i-r+k}, \ldots, x_{i+k}\}$, as

$$k \le l_0 + (r-2) - l \le l_0 + (r-2) - (r+1) = l_0 - 3,$$

and then the discontinuity does not cross it. In second case the stencil is $\{x_{i+l-(r-1)+k-r},$ $\ldots, x_{i+l-(r-1)+k}\}$, from

$$l - (r-1) + k \leq l - (r-1) + l_0 + (r-2) - l = l_0 - 1.$$

Using Proposition 4.4, the result is obtained. $\qquad\square$

LEMMA 5.4. *Let be* $1 < l_0 \leq r-1$. *If there exists a discontinuity at* $[x_{i+l_0-1}, x_{i+l_0}]$, *then*

$$(\tilde{C}_0^r, \tilde{C}_1^r, \ldots, \tilde{C}_{r-1}^r)$$
$$= \sum_{j_0=0}^{1} \tilde{\omega}_{0,j_0}^{r-2+l_0} \left(\sum_{j_1=j_0}^{j_0+1} \tilde{\omega}_{j_0,j_1}^{r-3+l_0} \left(\cdots \left(\sum_{j_{l_0-2}=j_{l_0-3}}^{j_{l_0-3}+1} \tilde{\omega}_{j_{l_0-3},j_{l_0-2}}^{r+1} \mathbf{C}_{\mathbf{j_{l_0-2}}}^{\mathbf{r+1}} \right) \cdots \right) \right) + O(h^{2mt})$$

with $\mathbf{C}_{\mathbf{k}}^{\mathbf{r+1}}$, $k = 0, \ldots, r-1$, *defined in* (31) *and*

$$(60) \qquad \tilde{\omega}_{k,k_1}^l = \frac{\tilde{\alpha}_{k,k_1}^l}{\tilde{\alpha}_{k,k}^l + \tilde{\alpha}_{k,k+1}^l}, \qquad \tilde{\alpha}_{k,k_1}^l = \frac{C_{k,k_1}^l}{(\epsilon + \tilde{I}_{k,k_1}^l)^t}, \quad k_1 = k, \ k+1,$$

where $\tilde{I}_{k,k_1}^l$ *are the smoothness indicators defined in section* 4.1, C_{k,k_1}^l *is defined in* (29), $m = 2$ *if the discontinuity is in the function, and* $m = 1$ *if the discontinuity is in the first derivative.*

Also,

(61)
$$(\tilde{\omega}_0^r, \tilde{\omega}_1^r, \ldots, \tilde{\omega}_{r-1}^r)$$
$$= (\hat{C}_0^r + O(h^{r-1}), \hat{C}_1^r + O(h^{r-1}), \ldots, \hat{C}_{l_0-1}^r + O(h^{r-1}), O(h^{2mt}), \ldots, O(h^{2mt})),$$

where

$$p_0^{l_0+r-1}\left(x_{i-\frac{1}{2}}\right) = \sum_{k=0}^{l_0-1} \hat{C}_k^r p_k^r \left(x_{i-\frac{1}{2}}\right).$$

Proof. Supposing that $1 < l_0 \leq r-1$, we can write

$$p_0^{l_0+r-1}\left(x_{i-\frac{1}{2}}\right) = \sum_{j_0=0}^{1} C_{0,j_0}^{l_0+r-2} p_{j_0}^{l_0+r-2}\left(x_{i-\frac{1}{2}}\right)$$

$$= \sum_{j_0=0}^{1} C_{0,j_0}^{l_0+r-2} \left(\sum_{j_1=j_0}^{j_0+1} C_{j_0,j_1}^{l_0+r-3} p_{j_1}^{l_0+r-3}\left(x_{i-\frac{1}{2}}\right) \right)$$

$$(62) \qquad = \sum_{j_0=0}^{1} C_{0,j_0}^{l_0+r-2} \left(\sum_{j_1=j_0}^{j_0+1} C_{j_0,j_1}^{l_0+r-3} \left(\cdots \left(\sum_{j_{l_0-2}=j_{l_0-3}}^{j_{l_0-3}+1} C_{j_{l_0-3},j_{l_0-2}}^{r+1} \right. \right. \right.$$
$$\left. \left. \left. \times \left(\sum_{j_{l_0-1}=j_{l_0-2}}^{j_{l_0-2}+1} C_{j_{l_0-2},j_{l_0-1}}^{r} p_{j_{l_0-1}}^{r}\left(x_{i-\frac{1}{2}}\right) \right) \right) \cdots \right) \right)$$

$$= \sum_{k=0}^{l_0-1} \hat{C}_k^r p_k^r \left(x_{i-\frac{1}{2}}\right).$$

Then, by (34) and Lemma 5.2,

$$(\tilde{C}_0^r, \tilde{C}_1^r, \ldots, \tilde{C}_{r-1}^r)$$

$$= \sum_{j_0=0}^{1} \tilde{\omega}_{0,j_0}^{r-2+l_0} \left(\sum_{j_1=j_0}^{j_0+1} \tilde{\omega}_{j_0,j_1}^{r-3+l_0} \left(\cdots \left(\sum_{j_{l_0-2}=j_{l_0-3}}^{j_{l_0-3}+1} \tilde{\omega}_{j_{l_0-3},j_{l_0-2}}^{r+1} \mathbf{C}_{\mathbf{j_{l_0-2}}}^{\mathbf{r+1}} \right) \cdots \right) \right) + O(h^{2mt}).$$

And by Lemmas 5.1 and 5.3, we obtain

$$(\tilde{\omega}_0^r, \tilde{\omega}_1^r, \ldots, \tilde{\omega}_{r-1}^r)$$
$$= (\hat{C}_0^r + O(h^{r-1}), \hat{C}_1^r + O(h^{r-1}), \ldots, \hat{C}_{l_0-1}^r + O(h^{r-1}), O(h^{2mt}), \ldots, O(h^{2mt})). \quad \square$$

THEOREM 5.5. *Let* $1 < l_0 \leq r - 1$ *and* $\tilde{\omega}_k^r$ *defined in* (35)*; if* f *is smooth in* $[x_{i-r}, x_{i+r-1}] \setminus \Omega$ *and* f *has a discontinuity at* Ω, *then*

(63) $$\sum_{k=0}^{r-1} \tilde{\omega}_k^r p_k^r \left(x_{i-\frac{1}{2}} \right) - f \left(x_{i-\frac{1}{2}} \right) = \left\{ \begin{array}{ll} O(h^{2r}) & if \ \Omega = \emptyset; \\ O(h^{r+l_0}) & if \ \Omega = [x_{i+l_0-1}, x_{i+l_0}]. \end{array} \right.$$

Proof. Let $1 < l_0 \leq r - 1$; then

$$\sum_{k=0}^{r-1} \tilde{\omega}_k^r p_k^r \left(x_{i-\frac{1}{2}} \right) - f \left(x_{i-\frac{1}{2}} \right)$$

$$= \sum_{k=0}^{r-1} \tilde{\omega}_k^r p_k^r \left(x_{i-\frac{1}{2}} \right) - p_0^{l_0+r-1} \left(x_{i-\frac{1}{2}} \right) + p_0^{l_0+r-1} \left(x_{i-\frac{1}{2}} \right) - f \left(x_{i-\frac{1}{2}} \right)$$

$$= \sum_{k=0}^{r-1} (\tilde{\omega}_k^r - \hat{C}_k^r) p_k^r \left(x_{i-\frac{1}{2}} \right) + O(h^{r+l_0})$$

$$= \sum_{k=0}^{l_0-1} (\tilde{\omega}_k^r - \hat{C}_k^r) \left(p_k^r \left(x_{i-\frac{1}{2}} \right) - f \left(x_{i-\frac{1}{2}} \right) \right) + \sum_{k=l_0}^{r-1} \tilde{\omega}_k^r p_k^r \left(x_{i-\frac{1}{2}} \right) + O(h^{r+l_0})$$

$$= O(h^{r-1+r+1}) + O(h^{2mt}) + O(h^{r+l_0})$$

$$= O(h^{r+l_0}). \qquad \qquad \square$$

Finally, if $l_0 = 1$, then the WENO classic interpolation is obtained and the order in the interval $[x_i, x_{i+1}]$ is $O(h^{r+1})$.

Now, let's try to determine the value of the parameter t in (8). The polynomial obtained with the new WENO technique must satisfy the following properties:
- It is a piecewise interpolation polynomial composed of polynomials of degree r.
- Every polynomial must satisfy the following property, which is equivalent to the *ENO property* [13], but that ensures a progressive order of accuracy:
  - The classical WENO weight related to any smooth stencil will verify

$$\tilde{\omega}_k^r = O(1).$$

  - If the function f has a singularity, then the corresponding $\tilde{\omega}_k^r$ will verify

$$\tilde{\omega}_k^r = O\left(h^{r-1}\right).$$

COROLLARY 5.6. *The new WENO algorithm satisfies the previous property if* $t \geq r$ *for jumps in the function and the first derivative.*

Proof. The proof is straightforward from (61) in Lemma 5.4. It can be seen that ensuring that $2mt \geq 2r - 1$ is enough. If $t = r$ the previous inequality is satisfied for jumps in the function or the first derivative. In fact, for jumps in the function it is enough if $t = ceil\left(\frac{2r-1}{2}\right)$, *ceil* being the operation of rounding to the upper closest integer. □

6. Numerical experiments. This section presents some numerical experiments used to test the theoretical results obtained in previous sections. In particular, the results related to the order of accuracy and the computational time of WENO-6, WENO-8, and WENO-10 algorithms are shown.

The accuracy will be checked through a grid refinement analysis. Let's consider the function

(64)
$$f(x) = \begin{cases} x^{10} - x^9 + x^8 - 4x^7 + x^6 + x^5 + x^4 + x^3 + 5x^2 + 3x, & a \leq x < 0, \\ \eta - (x^{10} - 2x^9 + 3x^8 - 8x^7 - 2x^6 + x^5 - 2x^4 - 3x^3 - 5x^2 + 0.5x), & 0 \leq x < b, \end{cases}$$

where η takes the values $\eta = 0, 1$. In the first case the function presents a discontinuity in the first derivative and in the second case a discontinuity in the function. Let's set $\eta = 0$ and consider the interval $(a, b) = (-\frac{\pi}{6}, 1 - \frac{\pi}{6})$. This configuration is chosen in order to force, if possible, that at all the stages of the grid refinement analysis, the singularity does not fall at a grid point. If the discontinuity does fall at a grid point, then the classical WENO strategy (or the new one) always provides an approximation of order $O(h^{r+1})$, as there is always one smooth stencil, and the grid refinement analysis does not show the real accuracy of the algorithms. If $\eta = 1$, then the interval $(a, b) = (-0.5, 0.5)$ can be considered. For all the experiments $t = r$ and $\epsilon = 10^{-16}$ have been chosen in (8) and (33) (greater values can be chosen for ϵ to obtain similar results, for example, $\epsilon = 10^{-10}$).

Tables 1 and 2 present a grid refinement analysis for the new WENO-6 and the classical WENO-6. Tables 3 and 4 present the same refinement analysis for the WENO-8 algorithms. Tables 5 and 6 present the results for the WENO-10 algorithms. All these tables have been obtained for the function in (64) with $\eta = 0$, which presents a jump in the first derivative.

Tables 7 and 8 (WENO-6), 9 and 10 (WENO-8), and 11 and 12 (WENO-10) show the same analysis but, in this case, for $\eta = 1$, so (64) presents a jump in the function.

In all the aforementioned tables 2^i initial points are used. The errors e_i are presented for interpolated data at grid points around the discontinuity. The interval that contains the discontinuity is always denoted as x_{2i}. It is clear that the accuracy is reduced step by step using the new algorithm. The classical WENO-2*r* algorithm is not capable of this adaption and typically attains $O(h^{r+1})$ accuracy at the interpolations whose stencils cross the discontinuity. Tables 3, 4, 5, 6, 9, 10, 11, and 12 only present complete results to the left of the discontinuity as the accuracy is symmetric. In order to obtain the computational time, 2000 executions of each subroutine are performed to obtain the mean. The computational times obtained show that the cost is similar for both algorithms for small values of r but that it slightly grows for the new algorithm as r grows.

7. Conclusions. In this work the algorithm introduced in [13, 14] has been generalized for data discretized in the point values. Explicit expressions for all the weights have been given and also a general proof that shows that the accuracy attained with this new WENO-2*r* strategy is optimal for any value of r. In addition,

TABLE 1
Grid refinement analysis for the new WENO-6 algorithm for the function in (64) and η = 0.

i	$\cdots x_{2i-7}$ e_i	$\log_2\left(\frac{e_i}{e_{i+1}}\right)$	x_{2i-5} e_i	$\log_2\left(\frac{e_i}{e_{i+1}}\right)$	x_{2i-3} e_i	$\log_2\left(\frac{e_i}{e_{i+1}}\right)$	x_{2i-1} e_i	$\log_2\left(\frac{e_i}{e_{i+1}}\right)$	x_{2i+1} e_i	$\log_2\left(\frac{e_i}{e_{i+1}}\right)$	x_{2i+3} e_i	$\log_2\left(\frac{e_i}{e_{i+1}}\right)$	$x_{2i+5}\cdots$ e_i	$\log_2\left(\frac{e_i}{e_{i+1}}\right)$	Comp. t.
5	1.575e-08	-	7.772e-09	-	5.103e-06	-	8.277e-03	-	1.690e-06	-	3.041e-08	-	2.846e-08	-	4.103e-04
6	1.477e-10	6.74	8.152e-10	3.25	4.968e-08	6.68	9.953e-03	-0.27	1.065e-07	3.99	2.929e-10	6.70	3.453e-10	6.36	5.570e-04
7	1.731e-12	6.41	3.586e-11	4.51	3.319e-09	3.90	1.764e-04	5.82	1.697e-05	-7.32	1.847e-08	-5.980	4.733e-12	6.19	6.398e-04
8	2.420e-14	6.16	1.205e-12	4.90	2.127e-10	3.96	1.764e-04	0	1.694e-08	9.97	1.168e-12	13.95	6.724e-14	6.14	1.056e-03
9	3.539e-16	6.10	3.884e-14	4.95	1.346e-11	3.98	1.764e-04	0	2.981e-11	9.15	3.656e-14	5	1.00e-15	6.07	1.816e-03
10	5.204e-18	**6.09**	1.232e-15	**4.98**	8.466e-13	**3.99**	1.761e-04	0.003	1.697e-12	**4.13**	1.198e-15	**4.93**	1.540e-17	**6.02**	3.411e-03

TABLE 2
Grid refinement analysis for the classical WENO-6 algorithm for the function in (64) and η = 0.

i	$\cdots x_{2i-7}$ e_i	$\log_2\left(\frac{e_i}{e_{i+1}}\right)$	x_{2i-5} e_i	$\log_2\left(\frac{e_i}{e_{i+1}}\right)$	x_{2i-3} e_i	$\log_2\left(\frac{e_i}{e_{i+1}}\right)$	x_{2i-1} e_i	$\log_2\left(\frac{e_i}{e_{i+1}}\right)$	x_{2i+1} e_i	$\log_2\left(\frac{e_i}{e_{i+1}}\right)$	x_{2i+3} e_i	$\log_2\left(\frac{e_i}{e_{i+1}}\right)$	$x_{2i+5}\cdots$ e_i	$\log_2\left(\frac{e_i}{e_{i+1}}\right)$	Comp. t.
5	1.574e-08	-	2.815e-07	-	9.477e-06	-	8.190e-03	-	1.712e-06	-	3.683e-07	-	2.851e-08	-	3.255e-04
6	1.477e-10	6.74	1.170e-08	4.59	5.403e-08	7.45	9.953e-03	-0.28	1.102e-07	3.96	2.454e-08	3.91	3.453e-10	6.37	3.326e-04
7	1.731e-12	6.41	7.822e-10	3.90	3.320e-09	4.02	1.764e-04	5.82	2.292e-05	-7.70	3.058e-07	-3.64	4.732e-12	6.19	5.427e-04
8	2.420e-14	6.16	4.963e-11	3.98	2.127e-10	3.96	1.764e-04	0	3.343e-08	9.42	8.320e-10	8.52	6.724e-14	6.14	9.487e-04
9	3.539e-16	6.10	3.124e-12	3.99	1.346e-11	3.98	1.764e-04	0	3.263e-11	10	6.540e-12	6.99	1.00e-15	6.07	1.605e-03
10	5.204e-18	**6.09**	1.959e-13	**3.99**	8.466e-13	**3.99**	1.757e-04	0.005	1.698e-12	**4.26**	3.921e-13	**4.06**	1.518e-17	**6.04**	2.860e-03

TABLE 3
Grid refinement analysis for the new WENO-8 algorithm for the function in (64) and η = 0.

i	$\cdots x_{2i-9}$ e_i	$\log_2\left(\frac{e_i}{e_{i+1}}\right)$	x_{2i-7} e_i	$\log_2\left(\frac{e_i}{e_{i+1}}\right)$	x_{2i-5} e_i	$\log_2\left(\frac{e_i}{e_{i+1}}\right)$	x_{2i-3} e_i	$\log_2\left(\frac{e_i}{e_{i+1}}\right)$	x_{2i-1} e_i	$\log_2\left(\frac{e_i}{e_{i+1}}\right)$	x_{2i+1} e_i	$\log_2\left(\frac{e_i}{e_{i+1}}\right)$	$x_{2i+3}\cdots$ e_i	$\log_2\left(\frac{e_i}{e_{i+1}}\right)$	Comp. t.
5	3.333e-11	-	1.963e-09	-	1.881e-08	-	2.532e-08	-	7.269e-03	-	3.938e-08	-	2.776e-08	-	3.450e-04
6	2.557e-13	7.03	1.275e-11	7.27	1.663e-10	6.82	2.061e-09	3.62	9.342e-03	-0.36	1.133e-09	5.12	3.104e-10	6.48	3.769e-04
7	6.106e-16	**8.71**	9.177e-14	7.12	1.713e-12	6.60	8.588e-11	4.58	1.543e-04	5.92	1.717e-06	-10.56	1.735e-08	-5.80	6.677e-04
8	6.939e-18	6.46	6.939e-16	7.05	2.212e-14	6.27	2.846e-12	4.92	1.543e-04	0	7.363e-11	14.51	4.880e-14	18.44	1.202e-03
9	0	-	5.204e-18	**7.06**	3.105e-16	6.15	9.115e-14	4.96	1.543e-04	0	8.792e-14	9.71	6.436e-16	6.24	2.141e-03
10	1.735e-18	-	0	-	4.337e-18	**6.16**	2.880e-15	**4.98**	1.539e-04	0.004	2.823e-15	**4.96**	9.324e-18	**6.11**	3.962e-03

TABLE 4

Grid refinement analysis for the classical WENO-8 algorithm for the function in (64) and η = 0.

i	x_{2i-9}		x_{2i-7}		x_{2i-5}		x_{2i-3}		x_{2i-1}		x_{2i+1}		$x_{2i+3}\cdots$		Comp. t.
	e_i	$\log_2\left(\frac{e_i}{e_{i+1}}\right)$	e_i	$\log_2\left(\frac{e_i}{e_{i+1}}\right)$	e_i	$\log_2\left(\frac{e_i}{e_{i+1}}\right)$	e_i	$\log_2\left(\frac{e_i}{e_{i+1}}\right)$	e_i	$\log_2\left(\frac{e_i}{e_{i+1}}\right)$	e_i	$\log_2\left(\frac{e_i}{e_{i+1}}\right)$	e_i	$\log_2\left(\frac{e_i}{e_{i+1}}\right)$	
5	4.966e-11	-	2.203e-09	-	4.532e-08	-	1.464e-07	-	7.246e-03	-	3.933e-08	-	2.134e-09	-	3.451e-04
6	2.583e-13	7.59	1.554e-10	3.82	5.618e-10	6.33	2.064e-09	6.15	9.341e-03	-0.37	1.136e-09	5.11	3.685e-10	2.53	3.563e-04
7	6.106e-16	**8.72**	5.924e-12	4.71	2.193e-11	4.68	8.588e-11	4.59	1.543e-04	5.92	4.457e-06	-11.94	4.902e-07	-10.38	6.170e-04
8	0	-	1.924e-13	4.94	7.171e-13	4.93	2.846e-12	4.92	1.543e-04	0	2.158e-10	14.33	1.420e-10	11.75	1.098e-03
9	0	-	6.113e-15	4.98	2.287e-14	4.97	9.115e-14	4.96	1.543e-04	0	8.977e-14	11.23	2.510e-14	12.47	1.928e-03
10	1.735e-18	-	1.926e-16	**4.99**	7.225e-16	**4.98**	2.880e-15	**4.98**	1.530e-04	0.01	2.823e-15	**4.99**	7.082e-16	**5.15**	3.458e-03

TABLE 5

Grid refinement analysis for the new WENO-10 algorithm for the function in (64) and η = 0.

i	x_{2i-11}		x_{2i-9}		x_{2i-7}		x_{2i-5}		x_{2i-3}		x_{2i-1}		$x_{2i}\cdots$		Comp. t.
	e_i	$\log_2\left(\frac{e_i}{e_{i+1}}\right)$	e_i	$\log_2\left(\frac{e_i}{e_{i+1}}\right)$	e_i	$\log_2\left(\frac{e_i}{e_{i+1}}\right)$	e_i	$\log_2\left(\frac{e_i}{e_{i+1}}\right)$	e_i	$\log_2\left(\frac{e_i}{e_{i+1}}\right)$	e_i	$\log_2\left(\frac{e_i}{e_{i+1}}\right)$	e_i	$\log_2\left(\frac{e_i}{e_{i+1}}\right)$	
5	1.762e-11	-	1.201e-11	-	2.408e-11	-	1.603e-10	-	3.584e-09	-	5.429e-08	-	7.261e-03	-	4.026e-04
6	3.969e-15	**12.12**	3.136e-15	**11.90**	2.054e-14	10.19	3.414e-13	8.87	2.284e-11	7.29	4.842e-10	6.81	9.331e-10	-0.36	4.504e-04
7	2.776e-17	7.16	1.388e-17	7.82	1.388e-17	**10.53**	9.853e-16	**8.44**	1.651e-13	7.11	5.031e-12	6.59	1.389e-04	6.07	8.849e-04
8	1.388e-17	1.00	6.939e-18	1.00	6.939e-18	1.00	1.388e-17	6.15	1.256e-15	7.04	6.553e-14	6.26	1.389e-04	0	1.561e-03
9	0	-	3.469e-18	1.00	3.469e-18	1.00	1.735e-18	3.00	6.939e-18	**7.50**	9.259e-16	6.145	1.389e-04	0	2.670e-03
10	3.469e-18	-	1.735e-18	1.00	0	-	1.735e-18	0	0	-	1.214e-17	**6.25**	1.377e-04	0.012	5.035e-03

TABLE 6

Grid refinement analysis for the classical WENO-10 algorithm for the function in (64) and η = 0.

i	x_{2i-11}		x_{2i-9}		x_{2i-7}		x_{2i-5}		x_{2i-3}		x_{2i-1}		$x_{2i}\cdots$		Comp. t.
	e_i	$\log_2\left(\frac{e_i}{e_{i+1}}\right)$	e_i	$\log_2\left(\frac{e_i}{e_{i+1}}\right)$	e_i	$\log_2\left(\frac{e_i}{e_{i+1}}\right)$	e_i	$\log_2\left(\frac{e_i}{e_{i+1}}\right)$	e_i	$\log_2\left(\frac{e_i}{e_{i+1}}\right)$	e_i	$\log_2\left(\frac{e_i}{e_{i+1}}\right)$	e_i	$\log_2\left(\frac{e_i}{e_{i+1}}\right)$	
5	1.683e-11	-	1.143e-11	-	9.436e-10	-	4.340e-09	-	1.873e-08	-	6.983e-08	-	7.263e-03	-	3.547e-04
6	3.886e-15	**12.08**	3.081e-15	**11.86**	8.765e-12	6.75	3.566e-11	6.93	1.081e-10	7.44	4.843e-10	7.17	9.331e-10	-0.36	3.896e-04
7	1.388e-17	8.13	0	-	9.374e-14	6.55	3.779e-13	6.56	1.135e-12	6.57	5.031e-12	6.59	1.389e-04	6.07	7.004e-04
8	1.388e-17	0	6.939e-18	-	1.263e-15	6.21	5.020e-15	6.23	1.493e-14	6.25	6.553e-14	6.26	1.389e-04	0	1.272e-03
9	0	-	0	-	1.735e-17	**6.19**	7.286e-17	**6.11**	2.134e-16	6.13	9.259e-16	6.14	1.389e-04	0	2.279e-03
10	0	-	1.735e-18	-	0	-	1.735e-18	5.39	3.469e-18	**5.94**	1.214e-17	**6.25**	1.351e-04	0.04	4.134e-03

TABLE 7
Grid refinement analysis for the new WENO-6 algorithm for the function in (64) and η = 1.

	$\cdots x_{2i-7}$		x_{2i-5}		x_{2i-3}		x_{2i-1}		x_{2i+1}		x_{2i+3}		$x_{2i+5}\cdots$		Comp. t.
i	e_i	$\log_2\left(\frac{e_i}{e_{i+1}}\right)$	e_i	$\log_2\left(\frac{e_i}{e_{i+1}}\right)$	e_i	$\log_2\left(\frac{e_i}{e_{i+1}}\right)$	e_i	$\log_2\left(\frac{e_i}{e_{i+1}}\right)$	e_i	$\log_2\left(\frac{e_i}{e_{i+1}}\right)$	e_i	$\log_2\left(\frac{e_i}{e_{i+1}}\right)$	e_i	$\log_2\left(\frac{e_i}{e_{i+1}}\right)$	
5	1.575e-08	-	7.924e-09	-	7.042e-07	-	4.343e-01	-	1.674e-06	-	3.041e-08	-	2.846e-08	-	3.716e-04
6	1.477e-10	6.74	8.152e-10	3.28	4.890e-08	3.85	4.579e-01	-0.08	1.057e-07	3.98	2.929e-10	6.70	3.453e-10	6.36	5.422e-04
7	1.731e-12	6.41	3.586e-11	4.51	3.319e-09	3.88	5.152e-01	-0.17	6.714e-09	3.98	2.432e-11	3.59	4.732e-12	6.19	6.678e-04
8	2.420e-14	6.16	1.205e-12	4.89	2.127e-10	3.96	5.078e-01	0.02	4.275e-10	3.97	1.046e-12	4.54	6.717e-14	6.14	1.051e-03
9	3.539e-16	6.10	3.884e-14	4.95	1.346e-11	3.98	5.041e-01	0.01	2.700e-11	3.98	3.653e-14	4.84	9.992e-16	**6.07**	1.810e-03
10	5.204e-18	**6.09**	1.232e-15	**4.98**	8.466e-13	**3.99**	5.022e-01	0.005	1.697e-12	**3.99**	1.221e-15	**4.90**	1.110e-16	3.17	3.411e-03

TABLE 8
Grid refinement analysis for the classical WENO-6 algorithm for the function in (64) and η = 1.

	$\cdots x_{2i-7}$		x_{2i-5}		x_{2i-3}		x_{2i-1}		x_{2i+1}		x_{2i+3}		$x_{2i+5}\cdots$		Comp. t.
i	e_i	$\log_2\left(\frac{e_i}{e_{i+1}}\right)$	e_i	$\log_2\left(\frac{e_i}{e_{i+1}}\right)$	e_i	$\log_2\left(\frac{e_i}{e_{i+1}}\right)$	e_i	$\log_2\left(\frac{e_i}{e_{i+1}}\right)$	e_i	$\log_2\left(\frac{e_i}{e_{i+1}}\right)$	e_i	$\log_2\left(\frac{e_i}{e_{i+1}}\right)$	e_i	$\log_2\left(\frac{e_i}{e_{i+1}}\right)$	
5	1.574e-08	-	1.560e-07	-	7.042e-07	-	4.634e-01	-	1.674e-06	-	3.665e-07	-	2.851e-08	-	3.186e-04
6	1.477e-10	6.74	1.163e-08	3.75	4.890e-08	3.85	4.742e-01	-0.03	1.057e-07	3.98	2.446e-08	3.91	3.453e-10	6.37	3.244e-04
7	1.731e-12	6.41	7.821e-10	3.90	3.319e-09	3.88	5.067e-01	-0.09	6.714e-09	3.98	1.560e-09	3.97	4.732e-12	6.19	5.479e-04
8	2.420e-14	6.16	4.963e-11	3.98	2.127e-10	3.96	5.035e-01	0.01	4.275e-10	3.97	9.912e-11	3.98	6.728e-14	6.14	9.495e-04
9	3.539e-16	6.10	3.124e-12	3.99	1.346e-11	3.98	5.019e-01	0.005	2.700e-11	3.98	6.247e-12	3.99	8.882e-16	**6.24**	1.602e-03
10	5.204e-18	**6.09**	1.959e-13	**3.99**	8.466e-13	**3.99**	5.011e-01	0.002	1.697e-12	**3.99**	3.920e-13	**3.99**	1.110e-16	3.00	2.869e-03

TABLE 9
Grid refinement analysis for the new WENO-8 algorithm for the function in (64) and η = 1.

	$\cdots x_{2i-9}$		x_{2i-7}		x_{2i-5}		x_{2i-3}		x_{2i-1}		x_{2i+1}		$x_{2i+3}\cdots$		Comp. t.
i	e_i	$\log_2\left(\frac{e_i}{e_{i+1}}\right)$	e_i	$\log_2\left(\frac{e_i}{e_{i+1}}\right)$	e_i	$\log_2\left(\frac{e_i}{e_{i+1}}\right)$	e_i	$\log_2\left(\frac{e_i}{e_{i+1}}\right)$	e_i	$\log_2\left(\frac{e_i}{e_{i+1}}\right)$	e_i	$\log_2\left(\frac{e_i}{e_{i+1}}\right)$	e_i	$\log_2\left(\frac{e_i}{e_{i+1}}\right)$	
5	3.333e-11	-	1.963e-09	-	1.881e-08	-	4.447e-09	-	3.636e-01	-	3.940e-08	-	2.776e-08	-	3.439e-04
6	2.557e-13	7.03	1.275e-11	7.27	1.663e-10	6.82	2.061e-09	1.11	4.152e-01	-0.19	1.133e-09	5.12	3.104e-10	6.48	3.855e-04
7	6.106e-16	**8.71**	9.178e-14	7.12	1.713e-12	6.60	8.588e-11	4.58	5.379e-01	-0.37	6.366e-11	4.15	3.810e-12	6.34	6.669e-04
8	6.939e-18	6.46	6.939e-16	7.05	2.212e-14	6.27	2.846e-12	4.92	5.194e-01	0.05	2.548e-12	4.64	4.741e-14	6.33	1.196e-03
9	0	-	5.204e-18	**7.06**	3.105e-16	6.15	9.115e-14	4.96	5.099e-01	0.03	8.682e-14	4.88	8.882e-16	**5.74**	2.107e-03
10	1.735e-18	-	0	-	4.337e-18	**6.16**	2.880e-15	**4.98**	5.051e-01	0.01	2.887e-15	**4.91**	1.110e-16	3.00	4.053e-03

TABLE 10
Grid refinement analysis for the classical WENO-8 algorithm for the function in (64) and $\eta = 1$.

i	x_{2i-9} e_i	$\log_2\left(\frac{e_i}{e_{i+1}}\right)$	x_{2i-7} e_i	$\log_2\left(\frac{e_i}{e_{i+1}}\right)$	x_{2i-5} e_i	$\log_2\left(\frac{e_i}{e_{i+1}}\right)$	x_{2i-3} e_i	$\log_2\left(\frac{e_i}{e_{i+1}}\right)$	x_{2i-1} e_i	$\log_2\left(\frac{e_i}{e_{i+1}}\right)$	x_{2i+1} e_i	$\log_2\left(\frac{e_i}{e_{i+1}}\right)$	$x_{2i+3}\cdots$ e_i	$\log_2\left(\frac{e_i}{e_{i+1}}\right)$	Comp. t.
5	4.966e-11	-	1.558e-09	-	4.137e-09	-	4.447e-09	-	4.455e-01	-	3.940e-08	-	2.211e-09	-	3.464e-04
6	2.583e-13	7.59	1.554e-10	3.33	5.605e-10	2.88	2.061e-09	1.11	4.653e-01	-0.06	1.133e-09	5.12	3.668e-10	2.59	3.598e-04
7	6.106e-16	**8.72**	5.924e-12	4.71	2.193e-11	4.68	8.588e-11	4.58	5.111e-01	-0.13	6.366e-11	4.15	1.692e-11	4.44	6.168e-04
8	0	-	1.924e-13	4.94	7.171e-13	4.93	2.846e-12	4.92	5.057e-01	0.01	2.548e-12	4.64	6.493e-13	4.70	1.102e-03
9	0	-	6.113e-15	4.98	2.287e-14	4.97	9.115e-14	4.96	5.030e-01	0.01	8.682e-14	4.87	2.220e-14	4.87	1.941e-03
10	1.735e-18	-	1.926e-16	**4.99**	7.225e-16	**4.98**	2.880e-15	**4.98**	5.016e-01	0.004	2.887e-15	**4.91**	7.772e-16	**4.84**	3.484e-03

TABLE 11
Grid refinement analysis for the new WENO-10 algorithm for the function in (64) and $\eta = 1$.

i	x_{2i-11} e_i	$\log_2\left(\frac{e_i}{e_{i+1}}\right)$	x_{2i-9} e_i	$\log_2\left(\frac{e_i}{e_{i+1}}\right)$	x_{2i-7} e_i	$\log_2\left(\frac{e_i}{e_{i+1}}\right)$	x_{2i-5} e_i	$\log_2\left(\frac{e_i}{e_{i+1}}\right)$	x_{2i-3} e_i	$\log_2\left(\frac{e_i}{e_{i+1}}\right)$	x_{2i-1} e_i	$\log_2\left(\frac{e_i}{e_{i+1}}\right)$	$x_{2i}\cdots$ e_i	$\log_2\left(\frac{e_i}{e_{i+1}}\right)$	Comp. t.
5	1.762e-11	-	1.201e-11	-	2.408e-11	-	1.603e-10	-	3.585e-09	-	5.425e-08	-	2.985e-01	-	3.937e-04
6	3.969e-15	**12.12**	3.136e-15	**11.90**	2.051e-14	10.20	3.414e-13	8.88	2.284e-11	7.29	4.842e-10	6.81	3.686e-10	-0.30	4.486e-04
7	2.776e-17	7.16	1.388e-17	7.82	1.388e-17	**10.53**	9.853e-16	**8.44**	1.651e-13	7.11	5.031e-12	6.59	5.640e-01	-0.61	8.132e-04
8	1.388e-17	1.00	6.939e-18	1.00	6.939e-18	1.00	1.388e-17	6.15	1.256e-15	7.04	6.553e-14	6.26	5.329e-01	0.08	1.486e-03
9	0	-	3.469e-18	-	3.469e-18	1.00	1.735e-18	3.00	6.939e-18	**7.50**	9.259e-16	6.14	5.167e-01	0.04	2.688e-03
10	0	-	1.735e-18	-	0	-	1.735e-18	0.00	0	-	1.214e-17	**6.25**	5.085e-01	0.02	5.044e-03

TABLE 12
Grid refinement analysis for the classical WENO-10 algorithm for the function in (64) and $\eta = 1$.

i	x_{2i-11} e_i	$\log_2\left(\frac{e_i}{e_{i+1}}\right)$	x_{2i-9} e_i	$\log_2\left(\frac{e_i}{e_{i+1}}\right)$	x_{2i-7} e_i	$\log_2\left(\frac{e_i}{e_{i+1}}\right)$	x_{2i-5} e_i	$\log_2\left(\frac{e_i}{e_{i+1}}\right)$	x_{2i-3} e_i	$\log_2\left(\frac{e_i}{e_{i+1}}\right)$	x_{2i-1} e_i	$\log_2\left(\frac{e_i}{e_{i+1}}\right)$	$x_{2i}\cdots$ e_i	$\log_2\left(\frac{e_i}{e_{i+1}}\right)$	Comp. t.
5	1.683e-11	-	1.143e-11	-	9.434e-10	-	3.901e-09	-	1.192e-08	-	5.425e-08	-	4.077e-01	-	3.564e-04
6	3.886e-15	**12.08**	3.081e-15	**11.86**	8.765e-12	6.75	3.566e-11	6.77	1.081e-10	6.78	4.842e-10	6.81	4.452e-01	-0.13	3.985e-04
7	1.388e-17	8.13	0	-	9.374e-14	6.55	3.779e-13	6.56	1.135e-12	6.57	5.031e-12	6.59	5.213e-01	-0.23	7.050e-04
8	1.388e-17	0	6.939e-18	-	1.263e-15	6.21	5.020e-15	6.23	1.493e-14	6.25	6.553e-14	6.26	5.109e-01	0.03	1.283e-03
9	0	-	0	-	1.735e-17	**6.19**	7.286e-17	**6.10**	2.134e-16	6.13	9.259e-16	6.145	5.056e-01	0.02	2.261e-03
10	0	-	1.735e-18	-	0	-	1.735e-18	5.39	3.469e-18	**5.94**	1.214e-17	**6.25**	5.029e-01	0.008	4.291e-03

we have proposed a strategy to use the smoothness indicators of order r, i.e., those used by the classical WENO algorithm, as smoothness indicators of high order, using a tree structure, in order to optimize the computational cost of the new algorithm. The numerical results presented support the theoretical conclusions reached. The numerical estimations of the computational times presented show that the new algorithm and the classical WENO algorithm perform very similarly.

REFERENCES

[1] X.-D. LIU, S. OSHER, AND T. CHAN, *Weighted essentially non-oscillatory schemes*, J. Comput. Phys., 115 (1994), pp. 200–212.

[2] G. JIANG AND C. W. SHU, *Efficient implementation of weighted ENO schemes*, J. Comput. Phys., 126 (1996), pp. 202–228.

[3] F. ARÀNDIGA, A. BAEZA, A. M. BELDA, AND P. MULET, *Analysis of WENO schemes for full and global accuracy*, SIAM J. Numer. Anal., 49 (2011), pp. 893–915.

[4] F. ARÀNDIGA, A.M. BELDA, AND P. MULET, *Point-value WENO multiresolution applications to stable image compression*, J. Sci. Comput., 43 (2010), pp. 158–182.

[5] A. K. HENRICK, T. D. ASLAM, AND J. M. POWERS, *Mapped weighted essentially non-oscillatory schemes: Achieving optimal order near critical points*, J. Comput. Phys., 207 (2005), pp. 542–567.

[6] M. CASTRO, B. COSTA, AND W. S. DON, *High order weighted essentially non-oscillatory WENO-Z schemes for hyperbolic conservation laws*, J. Comput. Phys., 230 (2011), pp. 1766–1792.

[7] C.-W. SHU, *Essentially Non-oscillatory and Weighted Essentially Non-oscillatory Schemes for Hyperbolic Conservation Laws*, Springer, Berlin, 1998, pp. 325–432.

[8] C.-W. SHU, *High order ENO and WENO schemes for computational fluid dynamics* in High-Order Methods for Computational Physics, Lect. Notes Comput. Sci. Eng. 9, Springer, Berlin, 1999, pp. 439–582.

[9] C.-W. SHU, *High order weighted essentially nonoscillatory schemes for convection dominated problems*, SIAM Rev., 51 (2009), pp. 82–126.

[10] C.-W. SHU AND Y.-T ZHANG, *ENO and WENO Schemes*, Elsevier/North-Holland, Amsterdam, 2016, pp. 103–122.

[11] A. HARTEN AND S. OSHER, *Uniformly high-order accurate nonoscillatory schemes. I*, SIAM J. Numer. Anal., 24 (1987), pp. 279–309.

[12] A. HARTEN, B. ENGQUIST, S. OSHER, AND S.R. CHAKRAVARTHY, *Uniformly high order accurate essentially non-oscillatory schemes*, III, J. Comput. Phys., 71 (1987), pp. 231–303.

[13] S. AMAT, J. RUIZ, AND C.-W. SHU, *On new strategies to control the accuracy of WENO algorithms close to discontinuities*, SIAM J. Numer. Anal., 57 (2019), pp. 1205–1237.

[14] S. AMAT, J. RUIZ, AND C-W. SHU, *On a new WENO algorithm of order $2r$ with improved accuracy close to discontinuities*, Appl. Math. Lett., 105 (2020), pp. 106–298.

[15] F. HU, *A Strategy Applied on WENO Interpolation to Improve the Accuracy Near Discontinuities*, preprint, ResearchGate, 2020.

[16] S. AMAT AND J. RUIZ, *New WENO smoothness indicators computationally efficient in the presence of corner discontinuities*, J. Sci. Comput., 71 (2017), pp. 1265–1302.

[17] M. ABRAMOWITZ AND I. A. STEGUN, *Handbook of Mathematical Functions with Formulas, Graphs, and Mathematical Tables*, Dover, New York, 2010.